



# Engineered dendritic cells-derived exosomes harboring HIV-1 Nef<sup>mut</sup>-Tat fusion protein and heat shock protein 70: A promising HIV-1 safe vaccine candidate

Parisa Moradi Pordanjani<sup>a</sup>, Azam Bolhassani<sup>a,\*</sup>, Mohammad Hassan Pouriayevali<sup>b</sup>,  
Alireza Milani<sup>a,c</sup>, Fatemeh Rezaei<sup>a</sup>

<sup>a</sup> Department of Hepatitis and AIDS, Pasteur Institute of Iran, Tehran, Iran

<sup>b</sup> Department of Arboviruses and Viral Hemorrhagic Fevers (National Reference Laboratory), Pasteur Institute of Iran, Tehran, Iran

<sup>c</sup> Iranian Comprehensive Hemophilia Care Center, Tehran, Iran

## ARTICLE INFO

### Keywords:

HIV-1 Nef<sup>mut</sup>-Tat protein  
Heat shock protein  
DC-based vaccine  
Exosome-based vaccine  
Electroporation  
Lentiviral vector

## ABSTRACT

Antigen presenting cells (APCs)-derived exosomes are nano-vesicles that can induce antigen-specific T cell responses, and possess therapeutic effects in clinical settings. Moreover, dendritic cells (DCs)-based vaccines have been developed to combat human immunodeficiency virus-1 (HIV-1) infection in preclinical and clinical trials. We investigated the immunostimulatory effects (B- and T-cells activities) of DCs- and exosomes-based vaccine constructs harboring HIV-1 Nef<sup>mut</sup>-Tat fusion protein as an antigen candidate and heat shock protein 70 (Hsp70) as an adjuvant in mice. The modified DCs and engineered exosomes harboring Nef<sup>mut</sup>-Tat protein or Hsp70 were prepared using lentiviral vectors compared to electroporation, characterized and evaluated by *in vitro* and *in vivo* immunological tests. Our data indicated that the engineered exosomes induced high levels of total IgG, IgG2a, IFN- $\gamma$ , TNF- $\alpha$  and Granzyme B. Moreover, co-injection of exosomes harboring Hsp70 could significantly increase the secretion of antibodies, cytokines and Granzyme B. The highest levels of IFN- $\gamma$  and TNF- $\alpha$  were observed in exosomes harboring Nef<sup>mut</sup>-Tat combined with exosomes harboring Hsp70 (Exo-Nef<sup>mut</sup>-Tat + Exo-Hsp70) regimen after single-cycle replicable (SCR) HIV-1 exposure. Generally, Exo-Nef<sup>mut</sup>-Tat + Exo-Hsp70 regimen can be considered as a promising safe vaccine candidate due to high T-cells (Th1 and CTL) activity and its maintenance against SCR HIV-1 exposure.

## 1. Introduction

An effective vaccine against human immunodeficiency virus-1 (HIV-1) infection should prevent infection completely or remove the infected CD4<sup>+</sup> T cells. Thus, it is critical to induce potent immune responses at the time of exposure to the virus [1,2]. Recently, extracellular vesicles (EVs) have been proposed as therapeutic agents to control viral infections. Exosomes (a main group of EVs)-based vaccines have demonstrated promising results against different types of infectious diseases *in vitro* and *in vivo* [3]. More than two decades ago, dendritic cells (DCs)-derived exosomes (named as DEXs) were developed to induce T-cell activity and co-stimulatory molecules, and finally tumor suppression. Exosomes-based vaccines possess an increased safety and improved half-life in blood circulation in comparison with other vaccines [4,5]. A variety of cells such as lymphocytes, mesenchymal stem cells (MSCs),

macrophages, dendritic cells (DCs) and tumor cells release exosomes with different contents. Exosomes are small membrane vesicles (30–150 nm in diameter) harboring cytoplasmic proteins (heat shock protein 70 (Hsp70) and Hsp90), cytoskeletal proteins (tubulin and actin), membrane fusion proteins (Rab GTPases) and membrane-associated proteins (CD9, CD81 and CD63) [6–8]. It was reported that exosomes secreted from immune cells are immunogenic and can elicit effective immune responses [9]. For instance, macrophages-derived exosomes carrying *Mycobacterium tuberculosis* antigens could induce the secretion of antigen-specific IFN- $\gamma$  and interleukin 2 (IL-2) [10]. Moreover, exosomes released from DCs have been used as an effective immunotherapy approach due to stability, safety, high biocompatibility, and contents (e.g., immune regulatory molecules) [11]. Antigen-pulsed DEXs could stimulate stronger antigen-specific immunity than microvesicles *in vivo* [12–14]. DEXs could also induce activation and proliferation of natural

\* Corresponding author.

E-mail address: [A\\_bolhassani@pasteur.ac.ir](mailto:A_bolhassani@pasteur.ac.ir) (A. Bolhassani).

<https://doi.org/10.1016/j.ijbiomac.2024.132236>

Received 23 March 2024; Received in revised form 4 May 2024; Accepted 7 May 2024

Available online 18 May 2024

0141-8130/© 2024 Elsevier B.V. All rights reserved.

killer (NK) cells by establishing interaction of the NKG2D ligand on DEXs with NKG2D receptors on the membrane of NK cells [15]. On the other hand, exosomes secreted by virus-infected cells (e.g., Influenza virus-infected cells in mice) could induce the secretion of cytokines and chemokines due to delivery of viral proteins and RNAs [16,17]. The studies showed that exosomes carrying the spike protein of SARS-CoV-2 elicited virus-specific neutralizing antibody titers [18,19]. Gould et al. proposed the “Trojan exosome” hypothesis because of the evolutionary similarity in biogenesis and transmission approaches between viruses and exosomes. This subject suggests the use of exosomes in vaccine design against viral infections (e.g., HIV, Ebola, influenza, hepatitis B and C viruses (HBV and HCV)) [20,21]. For example, the designed exosomes-based vaccines including Gp120-Exo or Gag-Exo (i.e., DEXs derived from DCs transfected with an adenoviral vector expressing envelope glycoprotein 120 (Gp120) or Gag) could activate antigen-specific cytotoxic T lymphocytes (CTLs) against HIV-1-infected cells in mice and animal models of chronic infection [22–24]. All studies indicated that the immunogenicity of exosomes depends on the amount and quality of antigens loaded in exosomes. Thus, new approaches are required to enhance the immunogenicity and therapeutic effects of exosomes-based vaccines [25]. Among HIV-1 proteins, Nef protein plays main roles in the survival of infected cells and vesicular trafficking [26]. It was reported that the mutant Nef protein (Nef<sup>mut</sup>) can be highly incorporated in exosomes. The Nef<sup>mut</sup> protein maintained the immunogenicity of wild type Nef, while lost its functions such as down-regulation of CD4<sup>+</sup> T cell and MHC class I, and enhancement of virus infectivity [25]. Moreover, the efficiency of Nef<sup>mut</sup> protein in exosomes was not significantly changed after linkage to the N-terminal region of foreign proteins (e.g., human papillomavirus (HPV)-16 E7) [25]. On the other hand, exosomes carry heat shock proteins such as Hsp20, Hsp27, Hsp70 and Hsp90 involved in antigen presentation, DC maturation, and translocation of NF- $\kappa$ B into the nucleus. The release of Hsp70 from human peripheral blood mononuclear cells (PBMCs) under natural and stress conditions showed immunogenic properties. The reports demonstrated the immunogenicity of exosomes may be related to the presence of Hsp70 and many main proteins for generation of immune responses (e.g., MHC-I, MHC-II, CD81, CD86 and CD11b) [27–30].

Up to now, different vaccines were designed based on the HIV-1 structural proteins (e.g., Env or Gag). Most of them couldn't significantly prevent the infection in *non-human primate* (NHP) models. To overcome these challenges, HIV-1 vaccines were developed based on the regulatory or accessory viral proteins (e.g., Tat/Rev./Nef) [31]. The viral Tat protein is an early regulatory protein with a variable length encoded by two exons (86–104 aa) [32]. Tat protein is highly conserved in the first 58 aa of exon 1 which plays a major role in the Tat transactivation activity [33,34]. In the current study, two engineered exosomes harboring the Nef<sup>mut</sup>-Tat fusion protein (Exo-Nef<sup>mut</sup>-Tat) and Hsp70 (Exo-Hsp70) were generated from mice bone marrow-derived DCs transduced with the lentivirions harboring the Nef<sup>mut</sup>-Tat protein or Hsp70 *in vitro*. After characterization of the engineered exosomes, *in vitro* cytokine secretion (IFN- $\gamma$ , TNF- $\alpha$ , and IL-10) was assessed by exposure of mice DCs and splenocytes (/ lymphocytes) to these exosomes. Moreover, exosomes-pulsed DCs were incubated with splenocytes (DCs + splenocytes) for evaluation of cytokine secretion *in vitro*. Then, mice immunization was performed by two main vaccination strategies including engineered exosomes-based vaccine constructs, and modified dendritic cells-based vaccine constructs. The humoral and cellular immune responses were evaluated using these vaccine constructs in mice. Finally, the pooled splenocytes isolated from each group were exposed to single-cycle replicable (SCR) HIV-1 for evaluating the secretion of cytokines *in vitro*. General overview of this study was shown in Graphical Abstract (as supplementary material).

## 2. Materials and methods

### 2.1. Construction of the recombinant plasmids

At first, the full length of human heat shock protein 70 kDa (HspA1A, Accession No: UniProtKB-P0DMV8), HIV-1 Nef (pNL4.3 vector, Accession No: AF324493.2) and HIV-1 Tat (pNL4.3 vector, Accession No: AF324493.2) were retrieved from the NCBI database. The mutations were considered in three nucleotides of Nef gene sequence containing G3C, V153L and E177G entitled as Nef<sup>mut</sup> [25]. The gene sequences of Nef<sup>mut</sup>-Tat (i.e., Nef<sup>mut</sup> linked to the exon I of Tat) and Hsp70 were designed in different vectors using SnapGene software, and synthesized in pUC57 cloning vector by GeneScript company. Then, for generation of pCDH-Hsp70 and pCDH-Nef<sup>mut</sup>-Tat, the Hsp70 and Nef<sup>mut</sup>-Tat transgenes were subcloned from pUC57 vector into the pCDH-CMV-MCS-EF1-copGFP-T2A-Puro (CD513B-1) eukaryotic expression vector using *NheI/BamHI* and *NheI/NotI* restriction enzymes (Fermentas, Germany), respectively. Also, for construction of pEGFP-Hsp70 and pEGFP-Nef<sup>mut</sup>-Tat, the Hsp70 and Nef<sup>mut</sup>-Tat gene fragments were subcloned into the pEGFP-N3 eukaryotic expression vector using *NheI/SalI* restriction enzymes (Fermentas, Germany). All recombinant vectors (pCDH-Hsp70, pCDH-Nef<sup>mut</sup>-Tat, pEGFP-Hsp70 and pEGFP-Nef<sup>mut</sup>-Tat) along with the psPAX2 (Plasmid #12260) and pMD2.G (Plasmid #12259) vectors (helper plasmids) for virion construction were prepared in large scale using an endotoxin-free plasmid DNA extraction Giga kit (Qiagen, Germany). Finally, the purity and concentration of DNA constructs were determined by NanoDrop Spectrophotometry.

### 2.2. Gene delivery of the recombinant vectors in mouse bone marrow-derived DCs

Gene delivery (/ transfection) in DCs was performed by two methods: a) electroporation using pEGFP-N3, pEGFP-Hsp70 and pEGFP-Nef<sup>mut</sup>-Tat; and b) lentiviral vectors using pCDH, pCDH-Hsp70 and pCDH-Nef<sup>mut</sup>-Tat. The goal of this study was to determine the most efficient delivery method with the highest protein expression.

### 2.3. Gene delivery in DCs using electroporation

Murine DCs were isolated from bone marrow according to the optimized protocol [35]. This study was approved by the Ethical Committee of Pasteur Institute of Iran with the code number of IR.PII.REC.1400.026. BALB/c mice (male, 5–7-week-old) were provided from Pasteur Institute of Iran. After anesthetizing with ketamine (50 mg/kg) and xylazine (10 mg/kg), the mice were sacrificed and immersed in 70 % ethanol. Briefly, bone marrow was flushed from the bone cavity of tibiae and femurs of male BALB/c mice. ACK lysis buffer (composed of NH<sub>4</sub>Cl, KHCO<sub>3</sub> and Na<sub>2</sub>EDTA; pH = 7.2, Sigma, Germany) was used to deplete erythrocytes. Then, the cells were cultured in complete medium (i.e., RPMI 1640 (Sigma, Germany) containing 20 % fetal bovine serum (FBS, Gibco, Germany), 3 % Penicillin-Streptomycin antibiotic (Sigma, Germany)) for 48 h to remove adherent macrophages. After that, non-adherent cells were cultured in culture medium containing 20 ng/mL of murine granulocyte-macrophage colony-stimulating factor (mGM-CSF; Pepro-Tech, Rocky Hill, USA) and 10 ng/mL of murine interleukin-4 (IL-4) (Pepro-Tech, Rocky Hill, USA). Culture medium was changed every 2 days, and cells were harvested on day 5. Immature DCs were stained to analyze surface expression of the DC markers including CD11c, MHC-II, CD86, CD40 and CD83 using FACScan Flow Cytometer (Becton Dickinson). The expression levels of CD11c, CD86, CD40, MHC-II and CD83 in immature DCs were 78.2 %, 52 %, 36 %, 61 % and 17.8 %, respectively. After DC isolation, the immature DCs were harvested, and centrifuged at 1200 rpm for 5 min. The cells were resuspended in 200  $\mu$ L of different buffers at a density of  $2 \times 10^6$  cells and added to the cuvettes after mixing with two concentrations (10  $\mu$ g and 2  $\mu$ g) of the plasmid DNA (i.e., pEGFP-Hsp70, pEGFP-Nef<sup>mut</sup>-Tat and pEGFP-N3).

The effects of voltage, number of pulses, concentration of plasmid and type of buffer were evaluated in ten experiments to determine the best transfection efficiency (Table 1) based on the published reports [36,37]. The electroporation was performed using Gene Pulser II Electroporation System (Bio-Rad, Richmond, CA). Then, the transfected DCs were diluted in 2 mL RPMI 1640 supplemented with 10 % FBS and Penicillin (100 U/mL)/Streptomycin (0.1 mg/mL), and transferred into a 12-well plate. Finally, the cells were incubated in a humidified 5 % CO<sub>2</sub> incubator at 37 °C for 48 h. Transfection efficiency was investigated using flow cytometry (Partec, Germany) and fluorescent microscopy.

#### 2.4. Gene delivery in mouse bone marrow-derived DCs using lentiviral vector

This experiment includes four steps as described in below: Cell culture, Production and titration of lentivirions, Transduction of DCs by lentiviral particles, and Evaluation of cytotoxic effects of polybrene for transduction of dendritic cells.

#### 2.5. Cell culture

The Lenti-X™ 293 T cell line (provided from the cell bank of Pasteur Institute of Iran) was grown in Dulbecco's Modified Eagle's Medium (DMEM; Gibco, Germany) supplemented with 10 % FBS and 1 % Penicillin-Streptomycin antibiotic. The cells were seeded at a density of  $4 \times 10^5$  cells in 6-well plate 24 h prior to transfection, and incubated under standard cell culture conditions (37 °C, 5 % CO<sub>2</sub>, humidified air) for achieving approximately 70 %–80 % confluency.

#### 2.6. Production and titration of lentivirions

For production of lentiviral particles (LVs), the lentiviral vectors containing transgenes (2 µg pCDH-Nef<sup>mut</sup>-Tat & pCDH-Hsp70) and without transgene) pCDH as a positive control (were co-transfected with pSPAX2 (1.5 µg) and pMD2.G (0.5 µg) into Lenti-X™ 293 T cells in a 6-well plate using TurboFect reagent (Fermentas, Germany) according to the manufacturer's protocol. The transfection efficiency was evaluated by flow cytometry and fluorescent microscopy at 24 h after transfection. Then, the cell supernatants were harvested at 48 and 72 h post-transfection, and were filtered through a 0.45 µm filter. After that, viral supernatants were concentrated by high speed centrifuge at 45000 g for 3 h. The concentrated supernatants were placed on a rocker at 4 °C for 24 h, and used for lentiviral titration. Briefly, a 12-well culture plate was seeded with HEK-293 T cells ( $1 \times 10^5$  cells/well; provided from the National Cell Bank, Pasteur Institute of Iran) in complete RPMI medium supplemented with 10 % FBS. After 24 h, the cells were harvested by trypsin and counted ( $350 \times 10^3$ ) to seed in the wells. The culture

medium was removed from each well, and 100 µL of 5-fold serial dilution of viral stock (the concentrated viral supernatants) was added to each well. Then, after 4–6 h, RPMI medium with 10 % FBS and 1 % Penicillin-Streptomycin antibiotic was added to each well. Finally, the percentage of transduced cells was determined by flow cytometry after 72 h. The following formula was used to determine viral titration:  $T = (N) \cdot (D) \cdot (P) / (V)$  [T: Titer (Unit/mL), P: Percentage of GFP positive cells, N: Number of cells, D: Dilution factor, V: Volume of virion solution]. In addition, for detection of the presence, size and morphology of lentiviral particles, the transmission electron microscopy (TEM) was used.

#### 2.7. Transduction of DCs by lentiviral particles

Murine DCs were generated as mentioned in the previous section. Then,  $5 \times 10^5$  cells were seeded in a non-treated 24-well plate and transduced with the recombinant lentivirions (MOI: 20) harboring Nef<sup>mut</sup>-Tat, Hsp70 and green fluorescent protein (GFP; without transgene) using 8 µg/mL polybrene reagent (Solarbio; contributing to lentivirion integration) according to the manufacturer's protocol. The cytotoxic effects of polybrene alone and combined with LVs on DCs were described in the next section. The infected cells were incubated in serum-free medium. Then, three hours after the cell transduction, the complete medium was added and incubated for 24 h at 37 °C in a humidified, 5 % CO<sub>2</sub> incubator. Next, medium was replaced with the pre-warmed exosome depleted complete medium (Thermo Fisher Scientific, UK) in the presence of 20 ng/mL murine GM-CSF and 10 ng/mL murine IL-4 cytokine. Finally, the transduction efficiency was investigated using fluorescent microscopy and flow cytometry at 48 h post-transduction.

#### 2.8. Evaluation of cytotoxic effects of polybrene for transduction of dendritic cells

Polybrene is a cationic polymer that improved the transduction efficiency of lentiviral particles in DCs *in vitro*. It has a neutralizing effect on negatively charged viral particles which facilitates their attachment and entry into DC cells. However, some cells are sensitive to polybrene, thus its cytotoxicity should be determined to improve cell transduction. At first, a serial dilution of the polybrene in incomplete RPMI medium was provided. Then, half of the polybrene solution was mixed with the lentiviral particles. Finally, the cytotoxic effects of polybrene alone and polybrene-LVs mixtures were evaluated on dendritic cells ( $5 \times 10^4$ ) seeded in a non-treated 96-well plate using MTT (3-(4, 5-dimethylthiazolyl-2)-2, 5 diphenyltetrazolium bromide, Sigma, Germany) for 24 h. Three formulations include: 1) different concentrations of polybrene, 2) different concentrations of polybrene along with different MOI of LVs added to each well, and 3) incubation of different concentrations of polybrene with different MOI of LVs for 2 h followed by the addition to

**Table 1**  
Optimization of gene delivery in DCs using electroporation under different conditions.

Program	Voltage	Number of cells	Plasmid	DNA Concentration	Type of buffer	Number of pulse	Pulse length
1	300 V	$2 \times 10^6$	pEGFP-Hsp70, pEGFP-Nef <sup>mut</sup> -Tat, pEGFP-N3	2 µg	RPMI*	1	5 ms
2	300 V	$2 \times 10^6$	pEGFP-Hsp70, pEGFP-Nef <sup>mut</sup> -Tat, pEGFP-N3	2 µg	RPMI	1	5 ms
3	300 V	$2 \times 10^6$	pEGFP-Hsp70, pEGFP-Nef <sup>mut</sup> -Tat, pEGFP-N3	2 µg	RPMI	1	1 ms
4	1300 V	$2 \times 10^6$	pEGFP-Hsp70, pEGFP-Nef <sup>mut</sup> -Tat, pEGFP-N3	2 µg	RPMI	2	1 ms
5	1300 V	$2 \times 10^6$	pEGFP-Hsp70, pEGFP-Nef <sup>mut</sup> -Tat, pEGFP-N3	10 µg	Buffer 1**	2	100 µs
6	600 V	$2 \times 10^6$	pEGFP-Hsp70, pEGFP-Nef <sup>mut</sup> -Tat, pEGFP-N3	10 µg	Buffer 1	1	5 ms
7	1300 V	$2 \times 10^6$	pEGFP-Hsp70, pEGFP-Nef <sup>mut</sup> -Tat, pEGFP-N3	10 µg	Buffer 2***	2	100 µs
8	600 V	$2 \times 10^6$	pEGFP-Hsp70, pEGFP-Nef <sup>mut</sup> -Tat, pEGFP-N3	10 µg	Buffer 2	2	5 ms
9	600 V followed by 1300 V	$2 \times 10^6$	pEGFP-Hsp70, pEGFP-Nef <sup>mut</sup> -Tat, pEGFP-N3	10 µg	Buffer 2	2	5 ms followed by 100 µs
10	1300 V followed by 600 V	$2 \times 10^6$	pEGFP-Hsp70, pEGFP-Nef <sup>mut</sup> -Tat, pEGFP-N3	10 µg	Buffer 2	2	100 µs followed by 5 ms

\* RPMI: Incomplete medium (without FBS).

\*\* Buffer 1: Standard isoosmolar electroporation medium: KH<sub>2</sub>PO<sub>4</sub>/K<sub>2</sub>HPO<sub>4</sub> (10 mM) + MgCl<sub>2</sub> (1 mM) + Sucrose (250 mM) with pH = 7.2

\*\*\* Buffer 2: Standard isoosmolar electroporation medium +20 % v/v incomplete RPMI.

each well (Table 2). The control sample contains un-treated DCs.

## 2.9. Isolation of DCs-derived engineered exosomes

Due to higher efficiency of DC transduction using lentiviral particles compared to electroporation, exosomes were isolated from DCs transduced with different lentivirions (Lenti-Nef<sup>mut</sup>-Tat, Lenti-Hsp70 and Lenti-GFP) at 72 h post-transduction. Moreover, exosomes were extracted from untransduced DCs. DCs-derived exosomes were isolated from the cell supernatants using ExoQuick-TC kit (System Biosciences) according to the manufacturer's protocol. After isolation, four solutions containing 4 types of pure exosomes were obtained and stored at -80 °C, named as empty exosome (Exo; DCs-derived exosomes), exosome-GFP (Exo-GFP; exosomes isolated from Lenti-GFP-transduced DCs), exosome-Hsp70 (Exo-Hsp70; exosomes isolated from Lenti-Hsp70-transduced DCs), and exosome-Nef<sup>mut</sup>-Tat (Exo-Nef<sup>mut</sup>-Tat; exosomes isolated from Lenti-Nef<sup>mut</sup>-Tat-transduced DCs). The total protein concentration of isolated exosomes was assessed using a bicinchoninic acid (BCA) protein assay kit (Thermo Fisher Scientific, USA) according to the manufacturer's instructions.

## 2.10. Characterization of DCs-derived exosomes

The size and morphology of the isolated exosomes were determined by transmission electron microscopy (TEM) using negative staining (LEO 906; Germany) at 100 kV. In addition, scanning electron microscopy (SEM, FEIESEM QUANTA 200-EDAX SILICON DRIFT) was used to detect the presence and surface morphology of the isolated exosomes. Zeta potential (surface charge) of exosomes was determined by Zetasizer (Nano ZS3600, Malvern Instruments, UK). On the other hand, western blotting was performed to identify exosomes through detection of CD63 and CD9 markers, and proteins loaded in exosomes (i.e., GFP, Nef<sup>mut</sup>-Tat and Hsp70). The anti-mouse CD63 monoclonal antibody (Abcam, USA; 1:1000 v/v), anti-mouse CD9 monoclonal antibody (Abcam, 1:500 v/v), anti-Nef monoclonal antibody (Abcam, 1:1000 v/v), anti-Hsp70 monoclonal antibody (Abcam, 1:1000 v/v), and anti-GFP polyclonal antibody (Abcam, 1:5000 v/v) were used to react with the proteins transferred to nitrocellulose membranes. All antibodies were conjugated to horseradish peroxidase (HRP); thus DAB (3, 3'-diaminobenzidine)/ hydrogen peroxide solution (Sigma, Germany) was used to detect the protein bands.

## 2.11. Preparation of the recombinant proteins

The recombinant (r) Nef<sup>mut</sup>-Tat protein and rHsp70 were previously prepared by our group (Department of Hepatitis and AIDS, Pasteur Institute of Iran, unpublished data). Herein, their expression was performed in large scale using isopropyl thiogalactopyranoside (IPTG; Sigma, Germany) inducer in the *E. coli* Rosetta (Nef<sup>mut</sup>-Tat protein) and BL21 (Hsp70) strains. They were produced in 16–18 h post-induction at 37 °C. The recombinant Nef<sup>mut</sup>-Tat (~35 kDa) and Hsp70 (~70 kDa) proteins were purified by affinity chromatography using Ni-NTA column under denaturing and native conditions according to Qiagen protocol, respectively and confirmed by sodium dodecyl sulfate-polyacrylamide gel electrophoresis (SDS-PAGE) technique. The purified proteins were

**Table 2**

Different formulations of polybrene for evaluation of its cytotoxicity on dendritic cells.

Formulation	Concentration of polybrene/ MOI of LVs			
1	8 µg/mL/	4 µg/mL/	2 µg/mL/	1 µg/mL/
	MOI = 0	MOI = 0	MOI = 0	MOI = 0
2	8 µg/mL/	4 µg/mL/	2 µg/mL/	1 µg/mL/
	MOI = 20	MOI = 10	MOI = 5	MOI = 2.5
3	8 µg/mL/	4 µg/mL/	2 µg/mL/	1 µg/mL/
	MOI = 20	MOI = 10	MOI = 5	MOI = 2.5

dialyzed against phosphate buffered saline 1 × (PBS1X), and assessed by NanoDrop spectrophotometry.

## 2.12. In vitro cytokine assay for evaluating potential immunostimulatory effects of exosomes

The immunostimulatory effects of engineered exosomes (Exo-Hsp70, Exo-Nef<sup>mut</sup>-Tat and Exo-GFP), and also rNef<sup>mut</sup>-Tat protein were evaluated on mouse bone marrow-derived DCs and mouse splenocytes (or lymphocytes) isolated from naive BALB/c mice (male, 5–7-week-old) using *in vitro* cytokine assay (i.e., IFN-γ, TNF-α, and IL-10). Moreover, mouse DCs pulsed with antigenic protein (rNef<sup>mut</sup>-Tat protein) and engineered exosomes were co-cultured with splenocytes, and the secretion of cytokines was investigated *in vitro*. The un-treated cells (DCs or splenocytes) were considered as control groups. Briefly, the immunostimulatory effects of exosomes or recombinant protein on acceptor DCs were investigated by incubating 10 µg exosomes or protein with 1 × 10<sup>6</sup> DCs. The morphological change was checked in the cells, and the culture supernatant was analyzed for cytokine secretion at 72 h post-incubation using a sandwich-based ELISA kit (Mabtech, Swedish Biotech Company) according to the manufacturer's instructions. Moreover, mouse splenocytes were investigated by incubating 10 µg exosomes or protein with 10 × 10<sup>6</sup> red blood cell depleted-splenocytes followed by harvesting on day 3 and measuring levels of cytokines using sandwich-based ELISA. On the other hand, exosomes/ protein-pulsed DCs (in 24 h) were cocultured in triplicates with splenocytes in a 96-well culture plate at a ratio of 1: 10 (number of cells: 1 × 10<sup>6</sup> DCs: 10 × 10<sup>6</sup> splenocytes) [38–40]. After 72 h, the secretion of cytokines was assessed by sandwich-based ELISA.

## 2.13. Mice immunization

Five to seven week old inbred BALB/c female mice were purchased from the breeding stocks maintained at Pasteur Institute of Iran. Five mice in each group were considered and immunized subcutaneously at the footpad with different formulations containing engineered exosomes (Exo-Nef<sup>mut</sup>-Tat, Exo-Hsp70, Exo-GFP), transduced DCs (DC-Nef<sup>mut</sup>-Tat, DC-Hsp70, DC-GFP), and the recombinant Nef<sup>mut</sup>-Tat protein (rNef<sup>mut</sup>-Tat) emulsified in Montanide 720 (Seppic S.A., France) at ratio of 30: 70 v/v (protein: adjuvant). The unmodified (or empty) DCs and exosomes (Exo), and PBS 1 × were used as control groups (Table 3). All experimental procedures were in accordance with the Animal Care and Use Protocol of Pasteur Institute of Iran (national guideline) for scientific purposes (Ethics code: IR.PII.REC.1400.026; Approval Date: 2021-06-07). Immunization was performed three times with a 2-week

**Table 3**

Immunization program in mice.

Group	Formulations	First injection (Prime: Day 0)	Second injection (Booster 1: Day 14)	Third injection (Booster 2: Day 28)
G1	DC-GFP	5 × 10 <sup>5</sup> cells	5 × 10 <sup>5</sup> cells	5 × 10 <sup>5</sup> cells
G2	Exo-GFP	10 µg	10 µg	10 µg
G3	DC-Nef <sup>mut</sup> -Tat	5 × 10 <sup>5</sup> cells	5 × 10 <sup>5</sup> cells	5 × 10 <sup>5</sup> cells
G4	Exo-Nef <sup>mut</sup> -Tat	10 µg	10 µg	10 µg
G5	Nef <sup>mut</sup> -Tat protein	10 µg	10 µg	10 µg
G6	+ Montanide	5 × 10 <sup>5</sup> cells	5 × 10 <sup>5</sup> cells	5 × 10 <sup>5</sup> cells
G7	DC-Hsp70	10 µg	10 µg	10 µg
G8	Exo-Hsp70	5 × 10 <sup>5</sup> cells	5 × 10 <sup>5</sup> cells	5 × 10 <sup>5</sup> cells
G9	DC-Nef <sup>mut</sup> -Tat +	+ 5 × 10 <sup>5</sup>	+5 × 10 <sup>5</sup> cells	+5 × 10 <sup>5</sup> cells
G10	DC-Hsp70	cells	10 µg + 10 µg	10 µg + 10 µg
G11	Exo-Nef <sup>mut</sup> -Tat +	10 µg + 10 µg	10 µg	10 µg
G12	Exo-HSP70	10 µg	40 µL	40 µL
	Empty Exosome (Exo)	40 µL	5 × 10 <sup>5</sup> cells	5 × 10 <sup>5</sup> cells
	PBS	5 × 10 <sup>5</sup> cells		
	Empty DC (DC)			

interval (Days 0, 14 & 28). The well-being of the animals was monitored daily, taking into consideration their appetite level, grooming behavior, general activity, and hair coat condition. Mice belonging to the same treatment group were housed together in polycarbonate cages maintained under controlled environmental conditions.

#### 2.14. Evaluation of antibody responses in mice sera

The pooled sera were prepared from each group, two weeks after the second injection and also three weeks after the third injection. The levels of antigen-specific total IgG and its subclasses (IgG1 and IgG2a) were determined in the pooled sera of each group (dilution: 1:100 v/v) using goat anti-mouse HRP-conjugated antibodies (dilution: 1:10000 v/v; Sigma, Germany) by indirect ELISA [41,42]. The coated antigens were rNef<sup>mut</sup>-Tat protein and rHsp70 (~5 µg/mL) diluted in PBS1X. Each sample was repeated in triplicate, and all results were shown as mean ± SD for each sample. Optical density was determined in 450 nm due to the use of 3, 3', 5, 5'-tetramethylbenzidine (TMB) as a substrate.

#### 2.15. Cytokine secretion assay

Three weeks after the last immunization, five mice from each group were sacrificed, and their spleen tissues were dissected. Then, the pooled splenocytes ( $2 \times 10^6$  cells/ well) without red blood cells (*i.e.*, lysed by ACK buffer) were cultured in 24-well plates containing complete RPMI-1640 medium supplemented with 10 % FBS, and re-stimulated with the recombinant proteins (5 µg/mL of Nef<sup>mut</sup>-Tat and Hsp70) for 72 h. A sample of each group without restimulation with antigens was included as a negative control. Moreover, concanavalin A (ConA) mitogen was used as a positive control. Finally, the cell supernatants were collected and stored in -70 °C. The secretion of IFN-γ, TNF-α and IL-10 in supernatants of the cultured splenocytes was assessed by a sandwich-based ELISA kit (Mabtech, Swedish Biotech Company) according to the manufacturer's instructions [41,42]. Each assay was repeated in duplicate and all results were shown as mean ± SD for each sample.

#### 2.16. Granzyme B secretion assay

The release of Granzyme B (or CTL activity *in vitro*) from effector splenocytes (E) was assessed by ELISA kit. Briefly, SP2/0 target cells (provided from the National Cell Bank, Pasteur Institute of Iran) were seeded in triplicate into U-bottomed 96-well plates ( $2 \times 10^4$  cells/well) for 24 h in the presence of 5 µg/mL of rNef<sup>mut</sup>-Tat protein and rHsp70. The pooled splenocytes of each group were added to the target cells at an E (splenocytes): T (SP2/0) ratio of 100:1 and co-cultured in RPMI1640 medium supplemented with 10 % heat-inactivated FBS at 37 °C and 5 % CO<sub>2</sub> under humidified conditions. After 6 h incubation, microplates were centrifuged at 250 g for 6 min at 4 °C, and the supernatants were harvested. The concentration of Granzyme B in these samples was measured using an ELISA kit (eBioscience, USA) according to the manufacturer's instructions [41,42]. Each assay was performed in triplicate. All results were shown as mean ± SD for each sample.

#### 2.17. Construction of SCR HIV-1 and cytokines secretion assay in infected immune cells

This experiment includes *in vitro* and *in vivo* assays as described in below:

a) *In vitro* assay: At first, SCR HIV-1 were generated *in vitro*. In brief, the HEK 293 T cells were seeded in a 6-well plate, and transfected with the lipofectamine 2000 transfection reagent (Sigma, Germany; 6 µL)/plasmid (4 µg of psPAX2, pmzNL4-3 and pMD2.G) complex. The produced virions were isolated from the cell supernatants using high speed centrifuge (45,000 g, 3 h) after 72 h, assessed by p24 ELISA assay kit (Cell Biolabs, USA), and stored at -70 °C [41]. Then, the

immunostimulatory effects of SCR HIV-1 (50 µg of p24 antigen) on naïve mice DCs, splenocytes, and SCR-pulsed DCs co-cultured with splenocytes were investigated by evaluating the secretion of IFN-γ, TNF-α and IL-10. The morphological change of SCR HIV-1 was investigated in DCs, as well.

b) *In vivo* assay: The pooled splenocytes of groups immunized with DC-Nef<sup>mut</sup>-Tat, Exo-Nef<sup>mut</sup>-Tat, DC-Nef<sup>mut</sup>-Tat + DC-HSP70, Exo-Nef<sup>mut</sup>-Tat + Exo-HSP70, Exo and DC (Table 3) were exposed to SCR HIV-1 (50 µg of p24 antigen) for 72 h. Then, the cell supernatants were collected to assess the secretion of IFN-γ, TNF-α and IL-10 using a sandwich-based ELISA kit [41]. Each assay was repeated in duplicate, and all results were shown as mean ± SD for each sample.

#### 2.18. Data analysis

The final results were statistically analyzed using one-way ANOVA to evaluate differences between groups (Prism 9.5.1, GraphPad Software, USA). Data were indicated as mean ± standard deviation (SD) for each group. A *p*-value <0.05 was statistically considered significant (\* *p* < 0.05; \*\* *p* < 0.01; \*\*\* *p* < 0.001; \*\*\*\* *p* < 0.0001; ns: non-significant (*p* > 0.05)).

### 3. Results

#### 3.1. Confirmation of the DNA constructs

The Hsp70 and Nef<sup>mut</sup>-Tat gene sequences were correctly subcloned in eukaryotic expression vectors (pCDH-CMV-MCS-E1-copGFP-T2A-Puro and pEGFP-N3). The presence of Hsp70 and Nef<sup>mut</sup>-Tat genes was confirmed using digestion as a clear band of ~1950 bp and ~ 893 bp migrated in agarose gel, respectively. The endotoxin-free recombinant plasmids (pCDH-Hsp70, pCDH-Nef<sup>mut</sup>-Tat, pEGFP-Hsp70 and pEGFP-Nef<sup>mut</sup>-Tat) had a concentration range of 2000–2700 ng/µL. The purity of plasmids was confirmed by the 260: 280 absorption ratios ranged from 1.8 to 1.9.

#### 3.2. Electro-transfection of the plasmid DNAs into DCs

The immature DCs were electro-transfected with pEGFP-Nef<sup>mut</sup>-Tat, pEGFP-Hsp70 and pEGFP-N3. Our results showed significant effects of voltage, DNA concentration, the number of pulse and buffer type on transfection efficiency. The programs of 5, 7 and 8 including 1300 V and 600 V versus 300 V, buffers 1 and 2 versus RPMI, 10 µg DNA versus 2 µg DNA, and 2 pulses versus 1 pulse showed higher DNA delivery than other conditions. The best transfection efficiency was quantified by flow cytometry about 19–35 % for the transfected DCs under conditions of 1300 V, 2 pulses of 100 µs, 10 µg DNA and buffer 1 (program 5, Table 4). The fluorescent microscopy images were shown for the best electroporation conditions (program 5), as well (Supplementary Fig. 1).

#### 3.3. Generation of the modified DCs

The lentiviral vectors harboring pCDH-Nef<sup>mut</sup>-Tat, pCDH-Hsp70 and pCDH were co-transfected with psPAX2 and pMD2.G plasmids (Helper plasmids) into Lenti-X™ 293 T cells using TurboFect reagent. The transfection efficiency was evaluated by fluorescent microscopy and flow cytometry at 24 h post-transfection. The transfection rates (or GFP positive populations) were 94.25 % ± 1.02, 87.1 % ± 0.60, and 96.0 % ± 2.33 for the cells transfected with pCDH-Nef<sup>mut</sup>-Tat, pCDH-Hsp70 and pCDH using flow cytometry analysis, respectively. The fluorescent microscopy images were shown in Supplementary Fig. 2. The supernatants were harvested at 48 and 72 h post-transfection, and the concentrated viral supernatants were confirmed by TEM images. The diameter of Lenti-GFP, Lenti-Nef<sup>mut</sup>-Tat and Lenti-Hsp70 particles was in a range of 80–100 nm (Supplementary Fig. 3). As observed, two copies of ssRNA enclosed by a capsid were observed in all lentiviral particles. After

lentivirions preparation, DCs were infected with them using polybrene (polybrene mixed with lentiviral particles and incubated for 2 h before adding to each well). The transduction efficiency was evaluated by fluorescent microscopy and flow cytometry at 72 h after DC transduction (Supplementary Fig. 4). The transduction rates (or GFP positive populations) in DCs transduced with Lenti-GFP, Lenti-Nef<sup>mut</sup>-Tat and Lenti-Hsp70 were 91.25 % ± 1.11, 91.33 % ± 0.50 and 90.2 % ± 1.03, respectively.

### 3.4. Cytotoxic effects of polybrene on DCs

The cytotoxic effects of three formulations of polybrene were evaluated on DCs using MTT assay in 570 nm by ELISA reader (Fig. 1). Generally, the results indicated that incubation of polybrene with lentivirions for 2 h and then their addition to DCs (formulation 3) increased cell viability significantly more than polybrene alone (formulation 1) and also polybrene + lentivirions (formulation 2). Indeed, the cytotoxic effects were considerably reduced in all polybrene concentrations and MOI of lentivirions. Moreover, the viability percentage was increased with the reduction of polybrene concentration and MOI of lentivirions. We used 8 µg/mL polybrene and MOI of 20 for lentivirions in transduction of DCs based on formulation 3 as described above. Although, lower amounts of polybrene and lentivirions (MOI) showed more cell viability; but the percentages of transduction were considerably lower than 8 µg/mL polybrene and MOI of 20 (62–71 % for 2 µg/mL polybrene and MOI of 5 versus 90–92 % for 8 µg/mL polybrene and MOI of 20). The viability rate of the control sample (*i.e.*, un-treated DCs) was 98.53 % ± 1.01.

### 3.5. Characterization and quantitation of exosomes

Isolation and identification of exosomes derived from the modified DCs were performed using SEM, TEM, DLS and western blotting. The results of SEM showed that the size of the nanovesicles was in a range of 50–80 nm in diameter. Moreover, ultra-structural analysis of the nanovesicles using TEM represented the typical spherical-shaped exosomes with a bilayer membrane (Fig. 2). The zeta potential (or surface charge) of exosomes detected by Zetasizer was -14.1 mV, 3.68 mV, 6.08 mV and 3.62 mV for Exo, Exo-GFP, Exo-Nef<sup>mut</sup>-Tat and Exo-Hsp70, respectively (Fig. 3) indicating positive charges of exosomes by the loaded proteins. It was interesting that the surface charge of Exo-Nef<sup>mut</sup>-Tat was more positive than Exo-GFP and Exo-Hsp70. On the other hand, western blotting was performed for detection of exosomal markers and the loaded proteins. The results showed the clear bands of ~26, ~53, ~35 and ~70 kDa for CD9, CD63, Nef<sup>mut</sup>-Tat and Hsp70, respectively confirming the correct nature of exosomes (*i.e.*, the presence of CD9 and CD63), and the proteins loaded in exosomes (*i.e.*, Nef<sup>mut</sup>-Tat and Hsp70) as shown in Supplementary Fig. 5. It should be mentioned that the empty exosome (Exo) showed a weak band of ~70 kDa for Hsp70 and no band for Nef<sup>mut</sup>-Tat protein. Moreover, the presence of CD9 and CD63 was detected in all exosomes (Exo, Exo-GFP, Exo-Nef<sup>mut</sup>-Tat and Exo-Hsp70) that was shown only once in Supplementary Fig. 5 due to the similarity of bands and prevention of repetition for each one

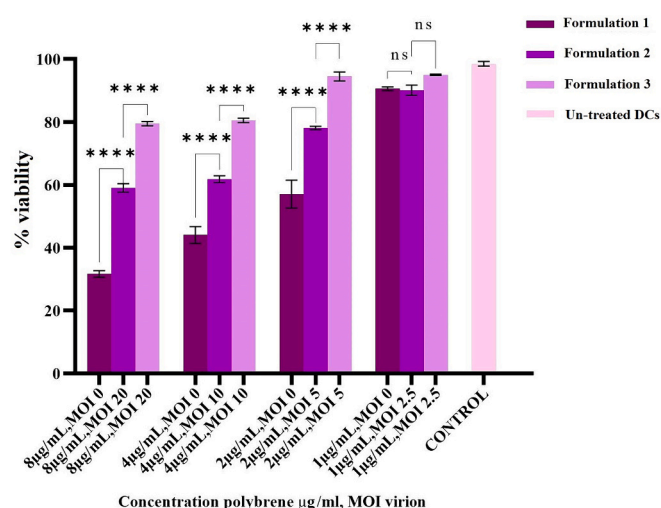


Fig. 1. The percentage of viability for DCs treated with polybrene (formulation 1), polybrene + LV (formulation 2) and polybrene incubated with LV for 2 h (formulation 3); ns: non-significant ( $p > 0.05$ ), \*\*\*\*:  $p < 0.0001$ .

individually. The total protein concentration of isolated exosomes was in a range of 0.5–0.8 µg/µL using BCA protein assay kit.

### 3.6. Generation of the recombinant proteins in large scale

The recombinant Nef<sup>mut</sup>-Tat protein (~35 kDa) and Hsp70 (~70 kDa) were prepared in large scale using affinity chromatography. We showed their expression and purification in Supplementary Fig. 6. The recombinant proteins (rNef<sup>mut</sup>-Tat and rHsp70) had a concentration range of 1.2–1.6 mg/mL.

### 3.7. In vitro cytokine secretion

The results of cytokines secretion from DCs incubated with different regimens such as the exosomes (Exo, Exo-GFP, Exo-Hsp70 and Exo-Nef<sup>mut</sup>-Tat) and the rNef<sup>mut</sup>-Tat protein showed a significant TNF-α response in comparison with other cytokines (*i.e.*, IFN-γ and IL-10;  $p < 0.0001$ ). It was interesting that the rNef<sup>mut</sup>-Tat-exposed DCs (G3) elicited higher levels of IL-10 than other groups ( $p < 0.0001$ ). All test groups (G1-G5) effectively enhanced the levels of TNF-α compared to control group (un-treated DCs, G6,  $p < 0.0001$ ; Fig. 4A). On the other hand, high levels of TNF-α were observed in all splenocytes exposed to different regimens (G1-G5) compared to control group (un-treated splenocytes, G6,  $p < 0.0001$ ). The highest levels of IFN-γ and IL-10 were observed in splenocytes exposed to rNef<sup>mut</sup>-Tat (G3) as compared to other groups ( $p < 0.0001$ ; Fig. 4B). Furthermore, interesting results for secretion of cytokines were obtained from different regimens-pulsed DCs co-cultured with splenocytes (DCs + splenocytes). As shown in Fig. 4C, Exo-Nef<sup>mut</sup>-Tat-pulsed DCs co-cultured with splenocytes (G2) could induce the highest level of IFN-γ as compared to other groups ( $p < 0.01$ ).

Table 4

Electro-transfection of the plasmid DNA into DCs.

Program	Voltage	Number of cells	Concentration of plasmid DNA	Type of buffer	Number of pulse	Pulse length	Transfection efficiency
5	1300 V	$2 \times 10^6$	10 µg	Buffer 1	2	100 µs	pEGFP-Hsp70 (19.2 %), pEGFP-Nef <sup>mut</sup> -Tat (32.8 %), pEGFP-N3 (35.1 %)
7	1300 V	$2 \times 10^6$	10 µg	Buffer 2	2	100 µs	pEGFP-Hsp70 (11.5 %), pEGFP-Nef <sup>mut</sup> -Tat (19.4 %), pEGFP-N3 (21.2 %)
8	600 V	$2 \times 10^6$	10 µg	Buffer 2	2	5 ms	pEGFP-Hsp70 (7.3 %), pEGFP-Nef <sup>mut</sup> -Tat (10.8 %), pEGFP-N3 (12.7 %)

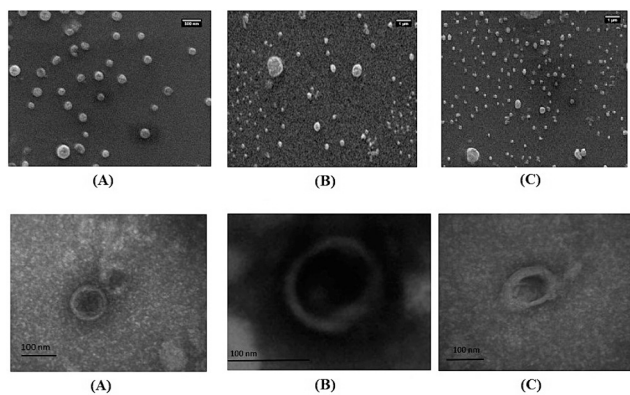


Fig. 2. Characterization of Exo-Nef<sup>mut</sup>-Tat (A), Exo-Hsp70 (B) and Exo-GFP (C) using SEM (above figures) and TEM (below figures) images.

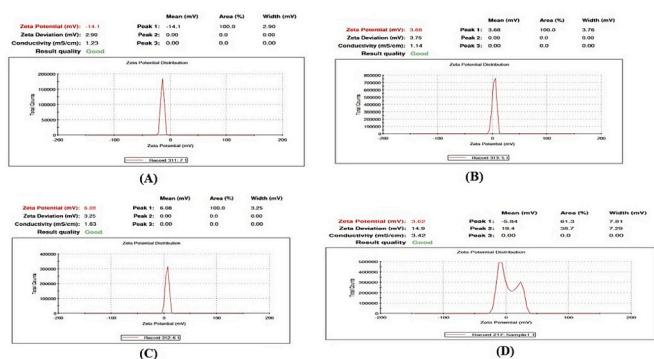


Fig. 3. Surface charge analysis of the nanovesicles using dynamic light scattering (DLS): Exo (A), Exo-GFP (B), Exo-Nef<sup>mut</sup>-Tat (C), Exo-Hsp70 (D).

The levels of TNF- $\alpha$  and IFN- $\gamma$  were significantly higher in all test groups (G1-G5) than control group (un-pulsed DCs + splenocytes, G6,  $p < 0.0001$ ). Generally, this experiment showed induction of cytokines from DCs and splenocytes isolated from naïve mice with different levels. The morphological changes of DCs occurred after exposure to Exo-Nef<sup>mut</sup>-Tat and Exo-Hsp70 as compared to other regimens (e.g., rNef<sup>mut</sup>-Tat) suggesting possible maturation of DCs (Fig. 4a-c). However, exact results of

antigen-specific immune responses were obtained from *in vivo* studies.

### 3.8. Cytokine secretion *in vivo*

The results of cytokines secretion from the pooled splenocytes of five mice in each group after restimulation with rNef<sup>mut</sup>-Tat protein (Fig. 5A) showed higher levels of IFN- $\gamma$  in groups receiving DC-Nef<sup>mut</sup>-Tat (G3), Exo-Nef<sup>mut</sup>-Tat (G4), DC-Nef<sup>mut</sup>-Tat + DC-Hsp70 (G8), Exo-Nef<sup>mut</sup>-Tat + Exo-HSP70 (G9) as compared to other groups ( $p < 0.0001$ ). In contrast, the highest level of TNF- $\alpha$  was detected in group receiving rNef<sup>mut</sup>-Tat protein (G5) as compared to other groups ( $p < 0.0001$ ). The level of IFN- $\gamma$  was significantly higher in groups immunized with DC-Nef<sup>mut</sup>-Tat (G3) and DC-Nef<sup>mut</sup>-Tat + DC-Hsp70 (G8) than groups immunized with Exo-Nef<sup>mut</sup>-Tat (G4) and Exo-Nef<sup>mut</sup>-Tat + Exo-HSP70 (G9) ( $p < 0.0001$ ). However, the levels of IFN- $\gamma$  and TNF- $\alpha$  did not show any significant differences between groups receiving DC-Nef<sup>mut</sup>-Tat (G3) and DC-Nef<sup>mut</sup>-Tat + DC-Hsp70 (G8), and also between groups receiving Exo-Nef<sup>mut</sup>-Tat (G4) and Exo-Nef<sup>mut</sup>-Tat + Exo-HSP70 (G9) ( $p > 0.05$ ) indicating antigen-specific immune responses. Moreover, all test groups (G1-G9) showed no significant levels of IL-10 in comparison with control groups (G10-G12;  $p > 0.05$ , Fig. 5A). On the other hand, the cytokines secretion was investigated in the pooled splenocytes after restimulation with rHsp70 for groups receiving Hsp70 in different formulations (Fig. 5B). The levels of IFN- $\gamma$  and TNF- $\alpha$  were higher in groups receiving Hsp70 (G6-G9) than other groups (G3, G4 and control groups;  $p < 0.0001$ ). Moreover, groups receiving DC-Nef<sup>mut</sup>-Tat + DC-Hsp70 (G8) and Exo-Nef<sup>mut</sup>-Tat + Exo-HSP70 (G9) showed higher levels of IFN- $\gamma$  and TNF- $\alpha$  than groups receiving DC-Hsp70 (G6) and Exo-Hsp70 (G7), respectively ( $p < 0.05$ ; Fig. 5B). Moreover, all test groups (G3, G4 and G6-G9) showed no significant levels of IL-10 in comparison with control groups (G10-G12;  $p > 0.05$ , Fig. 5B).

### 3.9. Evaluation of antibody responses

For evaluation of antibody responses, the levels of total IgG and the relevant subclasses were detected against rNef<sup>mut</sup>-Tat coated antigen using indirect ELISA. As observed in Fig. 6A, the highest levels of total IgG, IgG1 and IgG2a were observed in groups immunized with rNef<sup>mut</sup>-Tat protein (G5) as compared to other groups ( $p < 0.0001$ ). Moreover, groups immunized with DC-GFP (G1), Exo-GFP (G2), DC-Hsp70 (G6) and Exo-Hsp70 (G7) did not show any significant difference with control groups (G10-G12;  $p > 0.05$ ) indicating Nef<sup>mut</sup>-Tat antigen-specific antibody responses. Also, groups receiving Exo-Nef<sup>mut</sup>-Tat (G4) and

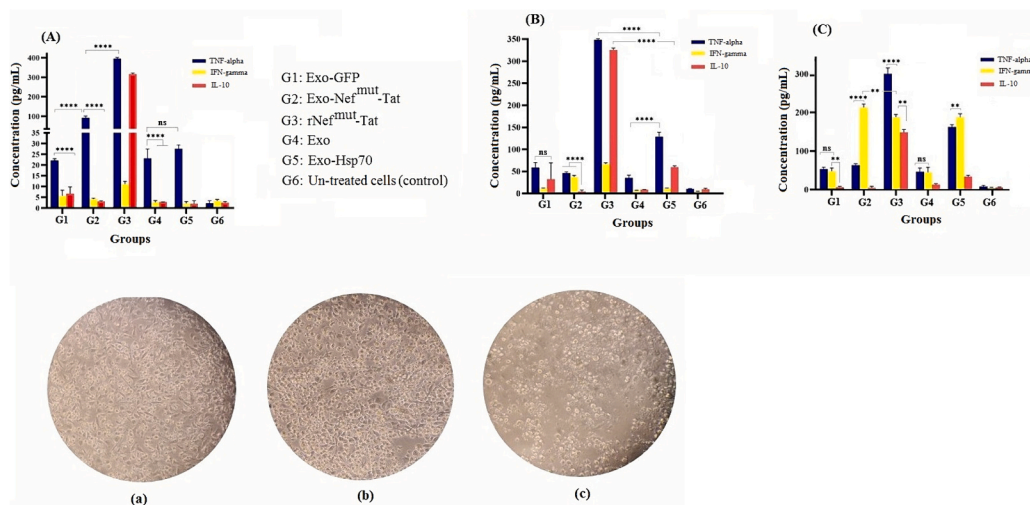
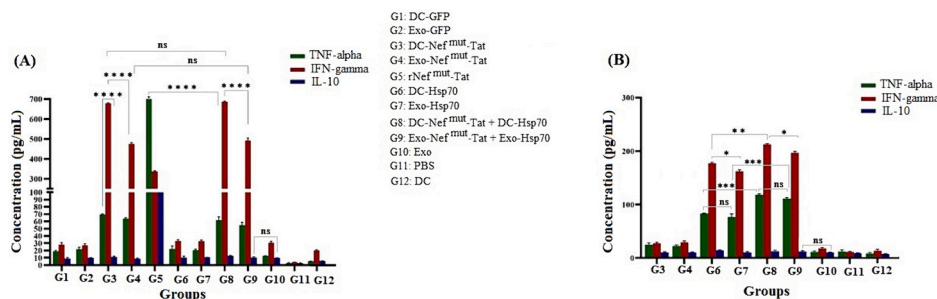
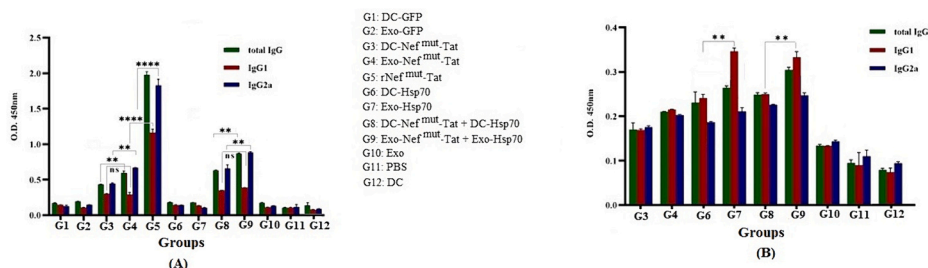


Fig. 4. Evaluation of *in vitro* cytokines secretion from naïve mice DCs (A), splenocytes (B) and DCs + splenocytes (C) exposed to different regimens (exosomes and recombinant protein) using a sandwich ELISA method; Morphological changes of DCs exposed to Exo-Nef<sup>mut</sup>-Tat (a), Exo-Hsp70 (b) and rNef<sup>mut</sup>-Tat protein (c); All analyses were performed in duplicate for each sample shown as mean absorbance at 450 nm  $\pm$  SD (ns: non-significant; \*\*  $p < 0.01$ ; \*\*\*\*  $p < 0.0001$ ).



**Fig. 5.** Evaluation of cytokines secretion in the pooled splenocytes of each group restimulated with rNef<sup>mut</sup>-Tat protein (A) and rHsp70 (B) using sandwich-based ELISA; All analyses were performed in duplicate for each sample shown as mean absorbance at 450 nm ± SD (ns: non-significant; \*  $p < 0.05$ ; \*\*  $p < 0.01$ ; \*\*\*  $p < 0.001$ ; \*\*\*\*  $p < 0.0001$ ).



**Fig. 6.** Evaluation of total IgG, IgG1 and IgG2a secretion against rNef<sup>mut</sup>-Tat protein (A) and rHsp70 (B) using indirect ELISA: All analyses were performed in duplicate for each sample shown as mean absorbance at 450 nm ± SD (ns: non-significant; \*\*  $p < 0.01$ ; \*\*\*\*  $p < 0.0001$ ).

Exo-Nef<sup>mut</sup>-Tat + Exo-Hsp70 (G9) induced higher total IgG and IgG2a than groups receiving DC-Nef<sup>mut</sup>-Tat (G3) and DC-Nef<sup>mut</sup>-Tat + DC-Hsp70 (G8), respectively ( $p < 0.01$ ). On the other hand, groups receiving Exo-Nef<sup>mut</sup>-Tat + Exo-Hsp70 (G9) and DC-Nef<sup>mut</sup>-Tat + DC-Hsp70 (G8) showed higher total IgG and IgG2a than groups receiving Exo-Nef<sup>mut</sup>-Tat (G4) and DC-Nef<sup>mut</sup>-Tat (G3), respectively indicating the importance of Hsp70 in stimulation of antibody responses ( $p < 0.001$ ). The data showed a mixture of IgG1 and IgG2a antibodies induced by groups receiving Exo-Nef<sup>mut</sup>-Tat (G4) and DC-Nef<sup>mut</sup>-Tat (G3) alone or along with Exo-Hsp70 (G9) and DC-Hsp70 (G8) directed more toward IgG2a. The high ratios of IgG2a to IgG1 showed direction toward Th1 cellular immunity. On the other hand, the levels of total IgG, IgG1 and IgG2a were not high in the immunized groups against rHsp70 coated antigen (Fig. 6B). However, among these groups, the highest levels of IgG1 were observed in mice immunized with Exo-Hsp70 (G7) and Exo-Nef<sup>mut</sup>-Tat + Exo-Hsp70 (G9) against the Hsp70 coated antigen ( $p < 0.01$ ).

### 3.10. Evaluation of Granzyme B secretion

Granzyme B secretion was measured in three weeks after the last injection in each group using ELISA. The data showed that among all the test groups, groups immunized with DC-Nef<sup>mut</sup>-Tat + DC-Hsp70 (G8) and Exo-Nef<sup>mut</sup>-Tat + Exo-Hsp70 (G9) produced significantly higher concentrations of Granzyme B than other groups ( $p < 0.001$ ) in response to the recombinant Nef<sup>mut</sup>-Tat protein. The Granzyme B secretion was significantly higher in groups immunized with Exo-Nef<sup>mut</sup>-Tat (G4) and Exo-Nef<sup>mut</sup>-Tat + Exo-Hsp70 (G9) compared to groups immunized with DC-Nef<sup>mut</sup>-Tat (G3) and DC-Nef<sup>mut</sup>-Tat + DC-Hsp70 (G8) in response to the recombinant Nef<sup>mut</sup>-Tat protein, respectively ( $p < 0.01$ ; Fig. 7A). On the other hand, the results of Granzyme B assay indicated that all the test groups had higher secretion of Granzyme B than control groups ( $p < 0.0001$ ) in response to the recombinant Hsp70 protein. The data showed that among all the test groups, groups immunized with DC-Nef<sup>mut</sup>-Tat + DC-Hsp70 (G8) and Exo-Nef<sup>mut</sup>-Tat + Exo-Hsp70 (G9) produced significantly higher concentration of Granzyme B than other groups ( $p < 0.05$ ) in response to the recombinant Hsp70 protein. However, no

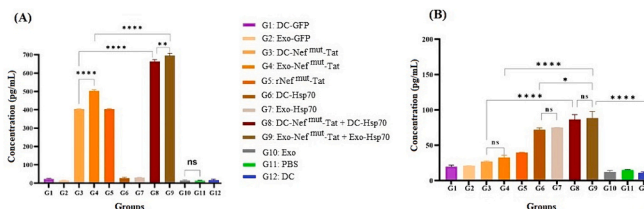


**Fig. 7.** Evaluation of granzyme B secretion in response to rNef<sup>mut</sup>-Tat protein (A) and rHsp70 (B) using sandwich-based ELISA; All analyses were performed in triplicate for each sample shown as mean absorbance at 450 nm ± SD (ns: non-significant; \*  $p < 0.05$ ; \*\*  $p < 0.01$ ; \*\*\*\*  $p < 0.0001$ ).

significant difference in Granzyme B secretion was observed between exosomes harboring Hsp70 (G7 and G9) and DCs harboring Hsp70 regimens (G6 and G8,  $p > 0.05$ ; Fig. 7B).

### 3.11. SCR effects on the secretion of cytokines from splenocytes

At first, we investigated the effects of SCR on the secretion of cytokines from DCs, splenocytes and DCs co-cultured with splenocytes, all isolated from Naive mice (Fig. 8A). The results of cytokines secretion from DCs showed high secretion of TNF- $\alpha$  as compared to control group (untreated DCs;  $p < 0.0001$ ). Moreover, high levels of IL-10, TNF- $\alpha$  and IFN- $\gamma$  were detected in splenocytes stimulated with SCR as compared to control group (unstimulated splenocytes;  $p < 0.0001$ ). It was interesting that the level of IL-10 was higher than TNF- $\alpha$  and IFN- $\gamma$  in splenocytes stimulated with SCR. In SCR-pulsed DCs co-cultured with splenocytes, the secretion of TNF- $\alpha$  and IFN- $\gamma$  from splenocytes was higher than SCR-stimulated splenocytes. However, no significant difference was observed in IL-10 secretion ( $p > 0.05$ ; Fig. 8A).

After mice immunization, the splenocytes of four groups including DC-Nef<sup>mut</sup>-Tat (G3), Exo-Nef<sup>mut</sup>-Tat (G4), DC-Nef<sup>mut</sup>-Tat + DC-Hsp70 (G8) and Exo-Nef<sup>mut</sup>-Tat + Exo-Hsp70 (G9) as well as control groups (G10-G12) were stimulated with SCR *in vitro* (Fig. 8B). The results

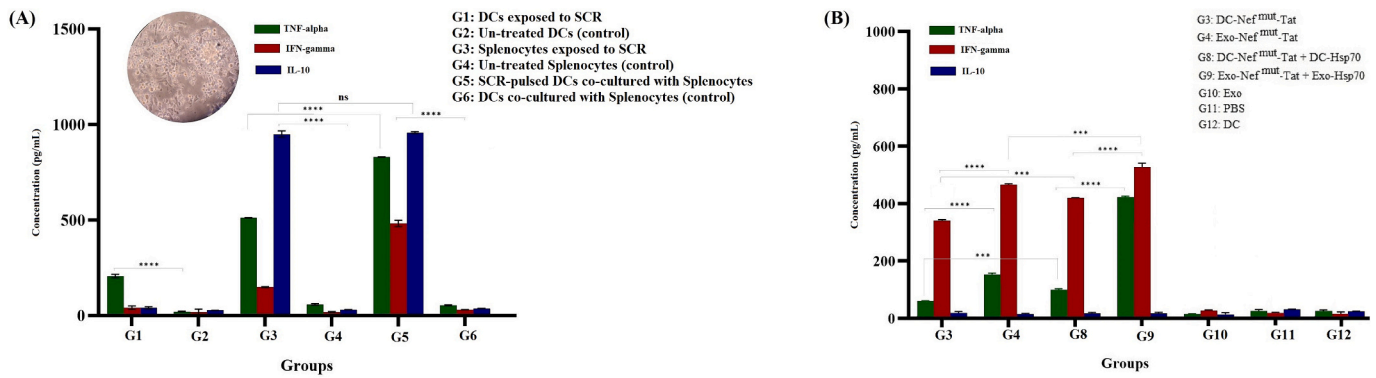


**Fig. 8.** Evaluation of IFN- $\gamma$ , TNF- $\alpha$  and IL-10 secretion in the DCs, splenocytes and DCs co-cultured with splenocytes isolated from Naïve mice *in vitro* along with morphological change of DCs exposed to virions (A), and in splenocytes isolated from immunized mice *in vitro* (B): All analyses were performed in duplicate for each sample shown as mean absorbance at 450 nm  $\pm$  SD (ns: non-significant; \*\*\*  $p < 0.001$ ; \*\*\*\*  $p < 0.0001$ ).

indicated that the secretion of TNF- $\alpha$  and IFN- $\gamma$  was higher than control groups (G10-G12;  $p < 0.0001$ ). Moreover, the levels of TNF- $\alpha$  and IFN- $\gamma$  were higher in groups immunized with exosomes (G4 and G9) than groups immunized with DCs (G3 and G8;  $p < 0.001$ ). It was interesting that the levels of IFN- $\gamma$  were increased in groups receiving exosomes (G4 and G9) and DCs (G3 and G8) as compared to the levels of TNF- $\alpha$  ( $p < 0.0001$ ). However, no considerable secretion of IL-10 was observed in all groups as compared to control groups. The highest levels of IFN- $\gamma$  and TNF- $\alpha$  were detected in group receiving Exo-Nef<sup>mut</sup>-Tat + Exo-Hsp70 (G9) among all groups (Fig. 8B).

#### 4. Discussion

The failure of strategies aimed at eradicating the HIV reservoirs is mainly related to the decreased expression of viral antigens in latently infected cells [43–45]. Recent studies have shown promising results of exosome-based therapy for development of HIV vaccines or diagnostic purposes [46]. Therapeutic vaccines should elicit strong Th1 and CTL responses to control HIV infection and eliminate infected cells [47]. The studies indicated that exosomes derived from pathogen-infected cells contain pathogen-specific antigens which can induce the proliferation of both CD4<sup>+</sup> and CD8<sup>+</sup> T cells [43,48,49]. Zitvogel et al. showed that DCs-derived exosomes could induce CD8<sup>+</sup> T cell-mediated anti-tumor immune response in mice [48]. Previous studies indicated that small EVs (*i.e.*, exosomes) induce Th1-type responses, while large EVs stimulate Th2-type responses [50–52]. For example, exosomes derived from *Salmonella*-infected cells induced a Th1-type response and increased *Salmonella*-specific CD4<sup>+</sup> T cell responses (*i.e.*, the release of IFN- $\gamma$ , IL-2 or TNF- $\alpha$ ) [50]. Cheng et al. showed that exosomes derived from macrophages treated with *Mycobacterium tuberculosis* induced antigen-specific IFN- $\gamma$  and IL-2-expressing CD4<sup>+</sup> and CD8<sup>+</sup> T cells [53,54]. Efforts are ongoing to evaluate the potential of exosomes-based vaccines against HIV infection [55]. However, potent and safe delivery of nucleic acids and proteins is a major issue in clinical settings. Different methods are utilized to deliver nucleic acids into the cells such as non-viral carriers (*e.g.*, electroporation and viral vectors). Electroporation was suggested as an effective, easy and low cost strategy for delivery of different cargos into the cells *in vivo* and *in vitro* [56]. Moreover, lentiviral vectors are other strong tools for gene delivery. They have some advantages including the ability to transduce non-dividing cells (*e.g.*, DCs), integration into the host cell genome for stable gene expression *in vitro* and *in vivo*, effective transduction in different tissues *in vivo* without toxicity or immune responses, and high gene delivery efficiency (95–100 %) [57–62].

Various factors influence the efficacy of electro-transfection including the number of pulses, intervals between pulses, voltage, cell type, and composition of electroporation buffer [63–65].

Electroporation buffer is an important factor responsible for cell viability after electroporation [66]. Thus, electroporation conditions should be optimized for different cell types. In this study, delivery of eukaryotic expression vectors harboring pEGFP-N3, pGFP-N3-Nef<sup>mut</sup>-Tat and pGFP-N3-Hsp70 into mouse bone marrow-derived DCs was evaluated using electroporation under different conditions. The highest percentage of electroporation efficiency for DCs (19–35 % with cell viability of  $\sim 80$  %) was obtained under conditions of 1300 V, 2 pulses of 100  $\mu$ s, 10  $\mu$ g DNA and standard buffer electroporation. Moreover, we used lentiviral vectors for gene delivery into DCs. Lentiviral particles (LVs) along with polybrene cationic polymer were used to transduce DCs after assessing cytotoxicity and finding the best formulation. The percentage of transduction efficiency was between 90 % and 92 % with high viability ( $\sim 90$  %). Thus, we used LVs for gene delivery into DCs (*i.e.*, preparation of modified DCs: DC-GFP, DC-Nef<sup>mut</sup>-Tat, DC-Hsp70), and subsequently isolation of the engineered exosomes (Exo-GFP, Exo-Nef<sup>mut</sup>-Tat, Exo-Hsp70). It was reported that extracellular vesicles (EVs) such as exosomes are negatively charged under physiological conditions that allows interaction of EVs with a positively charged molecule such as protamine to induce EV precipitation from serum, saliva and cell culture medium without the need for ultracentrifugation [67,68]. In our study, loading the Nef<sup>mut</sup>-Tat protein, Hsp70 and GFP in engineered exosomes was confirmed by western blotting as a clear band of  $\sim 35$  kDa (Exo-Nef<sup>mut</sup>-Tat),  $\sim 70$  kDa (Exo-Hsp70) and  $\sim 27$  kDa (Exo-GFP), respectively. Moreover, the results of surface charge of exosomes by zetasizer showed that Exo-Nef<sup>mut</sup>-Tat had a more positive surface charge than empty exosome (Exo) and other engineered exosomes (Exo-GFP and Exo-Hsp70). The surface charge of DCs-released exosomes is negative [69,70]; while the Nef<sup>mut</sup>-Tat protein has an overall positive charge determined by ProtParam (total number of negatively charged residues (Asp + Glu) was 32, and total number of positively charged residues (Arg + Lys) was 38). This result strengthens the anchoring of the Nef<sup>mut</sup>-Tat mosaic protein by the myristoyl and palmitoyl groups in the exosome membrane [25].

Viral infections induce a pro-inflammatory response including expression of cytokines [71]. Thus, some studies have investigated cytokine profiles in response to HIV vaccines [72]. For example, Huang et al. investigated a broad array of cytokines/chemokines produced in T-cell proliferation supernatants from a therapeutic HIV-1 vaccine clinical trial [73]. Some cytokines studied in HIV vaccines include IFN- $\gamma$ , TNF- $\alpha$ , and IL-10. IFN- $\gamma$  is produced by T cells and natural killer cells (NK cells) in response to viral infections. It has antiviral properties and is important for the control of viral replication [74]. Furthermore, the presence of IFN-stimulated genes such as ISG15, ISG56, MxB, OAS-1, GBP5 and Viperin with anti-HIV activity was reported in EVs. These genes code proteins with diverse functions aimed at blocking HIV [44]. On the other hand, TNF- $\alpha$  pro-inflammatory cytokine is produced by activated T cells

and macrophages. It plays a role in the immune response to viral infections, and can enhance the activity of other cytokines [74]. Lane et al. reported that TNF- $\alpha$  could suppress HIV-1 replication in bone marrow progenitors, blood monocytes and tissue macrophages through increasing the expression of the CCR5 ligand RANTES, and also decreasing the surface expression of the HIV-1 receptor CCR5 [75]. On the other hand, IL-10 anti-inflammatory cytokine is produced by regulatory T cells and other immune cells. It plays a role in the modulation of immune responses, and can suppress the activity of pro-inflammatory cytokines [74]. Herein, we evaluated the secretion of TNF- $\alpha$ , IFN- $\gamma$  and IL-10 from DCs, splenocytes (/ T-cells) and the pulsed DCs co-cultured with splenocytes. DCs have the unique capacity to activate naïve T cells by presenting T cell receptor-specific peptides from exogenously acquired antigens bound to MHC molecules [76]. Our results showed that Naïve mouse bone marrow-isolated DCs are capable of expressing diverse cytokine profiles (IFN- $\gamma$ , TNF- $\alpha$ , and IL-10) after exposure to exosomes (Exo, Exo-Nef<sup>mut</sup>-Tat, Exo-GFP, Exo-Hsp70) and rNef<sup>mut</sup>-Tat protein. The results showed that the Exo-Nef<sup>mut</sup>-Tat, Exo-GFP and Exo-Hsp70 regimens induced a higher secretion of TNF- $\alpha$  than IL-10 and IFN- $\gamma$ . As known, immature DCs do not produce IFN- $\gamma$  as observed in this study. On the other hand, the levels of IFN- $\gamma$  secreted from splenocytes were increased after co-culturing with DCs exposed to exosomes and rNef<sup>mut</sup>-Tat protein. Moreover, the levels of IL-10 were significantly lower in exosomes-exposed cells than in rNef<sup>mut</sup>-Tat protein-exposed cells. Indeed, the secretion of IFN- $\gamma$  and TNF- $\alpha$  from splenocytes was significantly lower than those from the pulsed DCs-co-cultured splenocytes. As known, mature T cells travel to tissue and organs in lymph system including spleen and lymph nodes [76]. According to the previous studies, T cell stimulators such as MHC-I, MHC-II and CD81 are available on exosome surfaces originating from APCs. The T stimulatory molecules play a critical role in antigen-specific interaction between B and T cells [77]. DCs-derived exosomes carry T cell co-stimulatory molecules (CD81) and T cell receptors on their surface to activate T-cells [53].

On the other hand, exosomes carry heat shock proteins such as Hsp20, Hsp27, Hsp70 and Hsp90 [53]. Our results showed that Exo-Hsp70 could induce higher levels of TNF- $\alpha$ , IFN- $\gamma$  and IL-10 in Naïve mice splenocytes co-cultured with DCs (DCs + splenocytes) as compared to Exo suggesting higher content of Hsp70 molecules in the engineered exosomes harboring Hsp70. Our findings confirmed the previous findings that the Hsp70 molecule offers adjuvant properties to exosomes [53]. Also, no significant difference in the secretion of cytokines from splenocytes co-cultured with DCs was observed between Exo-GFP and Exo. These findings suggested that the presence of GFP protein in the engineered exosomes (Exo-Nef<sup>mut</sup>-Tat, Exo-Hsp70) did not affect the results of cytokines secretion (or immunostimulatory properties). Previous studies also indicated that GFP lacks the ability to locate in exosomes [78]. GFP was further used to detect other proteins in exosomes [21,25].

In the current study, we also evaluated the humoral and cellular immune responses of Exo-Nef<sup>mut</sup>-Tat, Exo-Hsp70, Exo-GFP, Exo and Nef<sup>mut</sup>-Tat mosaic protein *in vivo*. As reported, the recipient DCs may interact with DEX through the endosomal pathway, and then the peptide-MHC complex is transferred to the DC surface membrane for antigen presentation to T-cell [53,79–81]. Moreover, the recipient DCs can uptake DEXs by facilitating membrane fusion and retain the peptide-MHC complex without processing on the DC surface. This mechanism of indirect antigen presentation was known as cross-dressing [81]. Kulkarni et al. showed an increased gene expression of the pro-inflammatory cytokines (IFN- $\gamma$  and TNF- $\alpha$ ), and activation of p38/Stat pathways in T-cells exposed to exosomes derived from HIV-1-infected DCs [82]. It was reported that DCs-derived exosomes can also activate NK cells [83]. Furthermore, the previous studies demonstrated that exosomes present antigens slowly *in vivo*, and their half-life can vary depending on various factors [84,85].

Our data showed that the splenocytes of mice immunized with DC-

Nef<sup>mut</sup>-Tat, Exo-Nef<sup>mut</sup>-Tat, DC-Nef<sup>mut</sup>-Tat + DC-Hsp70, and Exo-Nef<sup>mut</sup>-Tat + Exo-Hsp70 regimens after re-stimulation with Nef<sup>mut</sup>-Tat mosaic protein produced higher levels of IFN- $\gamma$  than other groups. The ratios of TNF- $\alpha$  and IFN- $\gamma$  to IL-10 in these groups were significantly higher than in other groups suggesting induction of Th1 cellular immune responses. The findings suggest that the balance between pro-inflammatory and anti-inflammatory cytokines is critical in determining the effectiveness of immunotherapeutic strategies [25,73,86]. For example, the immunological memory induced by DEXs was observed in CD4<sup>+</sup> T cells of mice treated with ovalbumin (OVA)-pulsed DEXs which elicited Th1 immune response [55,87]. Furthermore, our results indicated that group immunized with the recombinant Nef<sup>mut</sup>-Tat protein (G5) had the highest level of TNF- $\alpha$  and IL-10 among all groups. However, the secretion of IFN- $\gamma$  and the IFN- $\gamma$ /IL-10 ratio in group receiving rNef<sup>mut</sup>-Tat protein (G5) were lower than groups receiving DC-Nef<sup>mut</sup>-Tat (G3), Exo-Nef<sup>mut</sup>-Tat (G4), DC-Nef<sup>mut</sup>-Tat + DC-Hsp70 (G8), and Exo-Nef<sup>mut</sup>-Tat + Exo-Hsp70 (G9). Also, groups immunized with DC-Nef<sup>mut</sup>-Tat with or without DC-Hsp70 (G3 and G8) induced a higher level of IFN- $\gamma$  secretion than groups immunized with Exo-Nef<sup>mut</sup>-Tat with or without Exo-Hsp70 (G4 and G9). This result may be related to surface markers of DCs and more content of Nef<sup>mut</sup>-Tat protein in DCs. DCs as a common delivery system can control the direction of antigen-specific immune responses. However, DC vaccines are difficult to ensure standardized production, and lose efficacy over long periods of storage as compared to exosomes [77,88]. Due to these reasons, exosomes are recently proposed as a promising vaccine candidate. Our data indicated that group immunized with Exo-Nef<sup>mut</sup>-Tat + Exo-Hsp70 (G9) had a higher level of IFN- $\gamma$  than group immunized with Exo-Nef<sup>mut</sup>-Tat (G4) suggesting the adjuvant properties of Exo-Hsp70 as reported by Komarova et al. [30].

In the present study, the highest levels of antibodies (total IgG, IgG1 and IgG2a) against Nef<sup>mut</sup>-Tat coated antigen was observed in group immunized with rNef<sup>mut</sup>-Tat (G5) among all groups such as the engineered exosomes and modified DCs that may be related to more accessibility of free protein to B cells, the effect of Montanide 720 as an adjuvant, amount of protein, and importantly mechanism of antigen presentation. Our data showed that mice immunized with DC-Nef<sup>mut</sup>-Tat + DC-Hsp70 (G8) and Exo-Nef<sup>mut</sup>-Tat + Exo-Hsp70 (G9) increased the levels of total IgG and IgG2a in comparison with mice immunized with DC-Nef<sup>mut</sup>-Tat (G3) and Exo-Nef<sup>mut</sup>-Tat (G4), respectively. The higher presence of Hsp70 in Exo-HSP70 may enhance their ability to stimulate antibodies by promoting antigen presentation to immune cells. Moreover, the secretion of total IgG and IgG2a were higher in groups receiving Exo-Nef<sup>mut</sup>-Tat (G4) and Exo-Nef<sup>mut</sup>-Tat + Exo-Hsp70 (G9) than groups receiving DC-Nef<sup>mut</sup>-Tat (G3) and DC-Nef<sup>mut</sup>-Tat + DC-Hsp70 (G8). It should be mentioned that the ratio of IgG2a to IgG1 was significantly high in groups immunized with engineered exosomes (G4 and G9) and modified DCs (G3 and G8) indicating direction of immune responses toward Th1 immunity. The reports demonstrated that OVA-Dex helped accumulate the complement factors making the antigen epitopes more recognizable to B cells and thus inducing stronger IgG response. Similar to OVA-Dex, simultaneous pulsing of exosomes derived from BMDCs (Bone Marrow-derived Dendritic Cells) with  $\alpha$ GC could also amplify the titers of specific antibodies in a mouse model. In addition, B cells were crucial for the secondary expansion of CD8<sup>+</sup> T cells [13,89]. Segura et al. reported that the Dex could carry antigen-MHC complexes and ICAM1 molecules to B cells, thus promoting the stimulation of T cell *in vitro* and *in vivo* [2]. Qazi et al. showed that exosomes can provide antigens for B-cell activation, as indicated by the detection of IgG2a and IFN- $\gamma$  secretion from splenocytes [89]. *In vivo* studies using MUC1-Dex constructs have demonstrated high MUC1-specific IgG antibody titers with promotion of cytokine secretion. Additionally, CD8<sup>+</sup> T cells from immunized mice exhibited potent cytotoxicity against MUC1-positive tumor cells [90]. The studies established the presence of TNF receptors and ligands along with interferon-induced transmembrane proteins on exosome surfaces. It was

hypothesized that these exosomes can influence T and B cells [83,89]. Moreover, viral proteins loaded in EV-based vaccines could indirectly activate B cells and CD8<sup>+</sup> T cells through the cross-presentation of antigen [91]. From the previous findings, it can be concluded that exosomes are not only capable of stimulating B cells but also play a role in altering B cell function. The ratio of IgG2a to IgG1 can provide insights into the type of immune response, with an increased IgG1/IgG2a ratio indicating a Th2 type response and an increased IgG2a/IgG1 ratio suggesting a Th1 type response. However, the specific ratio of IgG2a to IgG1 in humoral immunity was not directly addressed in the search results [92,93].

On the other hand, CD8<sup>+</sup> cytotoxic T lymphocytes (CTLs) play a critical role in control of HIV-1 proliferation. Indeed, cellular immunity plays an important role in controlling the acute phase of infection and disease progression even in the absence of neutralizing antibodies [94–96]. Based on previous studies, exosomes engineered by Nef<sup>mut</sup> linked to viral proteins (HPV E7) were able to effectively stimulate CTLs [21,25]. Granzyme B (GrB) is a serine protease that plays a crucial role in the cytotoxic activity of CTLs and NK cells [97,98]. EVs can be engineered to display viral antigens and so induce high and specific CD8<sup>+</sup> T cells [87,99]. Herein, the secretion of Granzyme B was significantly increased in groups immunized with the Exo-Nef<sup>mut</sup>Tat + Exo-Hsp70 (G9) as compared to group immunized with the Exo-Nef<sup>mut</sup>Tat (G4). The same result was observed in regimens with modified DCs (G3 and G8) indicating the adjuvant effect of Hsp70 in these constructs. Moreover, the engineered exosomes (G4 and G9) showed higher Granzyme B secretion than modified DCs (G3 and G8). Krupka et al. reported that the levels of HIV antigen-specific IFN- $\gamma$  and Granzyme B secretion elicited by immunization with HSPs/HIV protein complexes were significantly higher than groups immunized with HIV proteins without HSPs molecules [100]. Among HSPs, Hsp70 was known as an effective adjuvant in vaccine development studies [12]. Another group reported that Hsp70 derived from TEXs (exosomes derived from tumor cells) activates NK cells leading to tumor cell lysis through Granzyme B secretion [101].

In the recent study, we reported the secretion of cytokines from splenocytes of immunized mice with engineered exosomes and modified DCs after exposure to SCR HIV-1. These results showed that unstimulated splenocytes of groups immunized with engineered exosomes (G4 and G9) significantly increased the secretion of IFN- $\gamma$  and TNF- $\alpha$  as compared to those of groups immunized with modified DCs (G3 and G8). Moreover, the secretion of IFN- $\gamma$  and TNF- $\alpha$  was higher in groups receiving Exo-Nef<sup>mut</sup>Tat + Exo-Hsp70 (G9) and DC-Nef<sup>mut</sup>Tat + DC-Hsp70 (G8) than Exo-Nef<sup>mut</sup>Tat (G4) and DC-Nef<sup>mut</sup>Tat (G3) indicating the immunostimulatory effects of Hsp70 as an adjuvant. Thus, the SCR HIV-1 could likely stimulate memory T cells indicating the maintenance of T cell activity in immunized mice.

## 5. Conclusions

The novelty and importance of this study include: a) Production and validation of engineered exosomes from DCs transduced with novel mosaic antigen (Nef<sup>mut</sup>-Tat) capable of presenting epitopes on the surface of exosomes; b) Evaluation of the role of Hsp70 as an adjuvant in engineered exosome platform; c) Evaluation of the cytotoxic effects of polybrene on DCs; d) Comparison of electroporation and lentiviral vectors in gene delivery; e) Comparison of the efficiency of modified DCs with engineered exosomes in immune stimulation, e) Evaluation of cytokines secretion *in vitro* and *in vivo*, and f) Comparison of the efficiency of modified DCs with engineered exosomes after exposure to SCR HIV-1 *in vitro*.

In summary, based on the obtained data, the high levels of IgG2a, IFN- $\gamma$ , TNF- $\alpha$  and Granzyme B secretion were observed in group receiving Exo-Nef<sup>mut</sup>Tat + Exo-Hsp70 suggesting induction of cellular immune response (Th1 and CTL activity). Although group receiving DC-Nef<sup>mut</sup>Tat + DC-Hsp70 induced higher IFN- $\gamma$  secretion than group

receiving Exo-Nef<sup>mut</sup>Tat + Exo-Hsp70, but it produced lower levels of IgG2a and Granzyme B. Moreover, it was important that the highest levels of IFN- $\gamma$  and TNF- $\alpha$  were detected in splenocytes of mice immunized with Exo-Nef<sup>mut</sup>Tat + Exo-Hsp70 after exposure to SCR HIV-1. Although splenocytes of group receiving DC-Nef<sup>mut</sup>Tat + DC-Hsp70 indicated considerable immune responses before and after exposure to SCR HIV-1; however, immunity induced by Exo-Nef<sup>mut</sup>Tat + Exo-Hsp70 was higher than other groups as well as safety, long-term storage and cell-free (virus-free) construct of exosomes. However, further studies are required to test these constructs in animal models (e.g., macaque).

Supplementary data to this article can be found online at <https://doi.org/10.1016/j.ijbiomac.2024.132236>.

## CRediT authorship contribution statement

**Parisa Moradi Pordanjani:** Writing – review & editing, Writing – original draft, Project administration, Investigation, Formal analysis. **Azam Bolhassani:** Writing – review & editing, Writing – original draft, Validation, Supervision, Project administration, Methodology, Investigation, Conceptualization. **Mohammad Hassan Pouriayevali:** Writing – review & editing, Project administration, Investigation. **Alireza Milani:** Writing – review & editing, Project administration, Investigation. **Fatemeh Rezaei:** Writing – review & editing, Investigation.

## Declaration of competing interest

The authors declare that they have no known competing financial interests or personal relationships that could have appeared to influence the work reported in this paper.

## Data availability

Data are available in the manuscript and supplementary files.

## Acknowledgments

Parisa Moradi Pordanjani was supported by Pasteur Institute of Iran, Tehran, Iran to pursue her study in the Ph.D. thesis.

## Ethics approval

All experimental procedures for animal studies were in accordance with the Animal Care and Use Protocol of Pasteur Institute of Iran (national guideline) for scientific purposes (Ethics code: IR.PII.REC.1400.026; Approval Date: 2021-06-07).

## References

- [1] M. Rubens, V. Ramamoorthy, A. Saxena, N. Shehadeh, S. Appunni, HIV vaccine: recent advances, current roadblocks, and future directions, *J. Immunol. Res.* 2015 (2015) 560347.
- [2] E. Segura, C. Nicco, B. Lombard, P. Véron, G. Raposo, F. Batteux, S. Amigorena, C. Théry, ICAM-1 on exosomes from mature dendritic cells is critical for efficient naive T-cell priming, *Blood* 106 (1) (2005) 216–223.
- [3] M. Negahdaripour, B. Vakili, N. Nezafat, Exosome-based vaccines and their position in next generation vaccines, *Int. Immunopharmacol.* 113 (2022) 109265.
- [4] N. Javeed, D. Mukhopadhyay, Exosomes and their role in the micro-/macro-environment: a comprehensive review, *J. Biomed. Res.* 31 (5) (2017) 386.
- [5] M. Cacciottolo, J.B. Nice, Y. Li, M.J. LeClaire, R. Twaddle, C.L. Mora, S.Y. Adachi, E.R. Chin, M. Young, J. Angeles, K. Elliott, M. Sun, Exosome-based multivalent vaccine: achieving potent immunization, broadened reactivity, and strong T-cell responses with nanograms of proteins, *Microbiology Spectrum* 11 (3) (2023) e00503–e00523.
- [6] A. Muntasell, A.C. Berger, P.A. Roche, T cell-induced secretion of MHC class II-peptide complexes on B cell exosomes, *EMBO J.* 26 (19) (2007) 4263–4272.
- [7] C. Admyre, S.M. Johansson, S. Paulie, S. Gabriellsson, Direct exosome stimulation of peripheral human T cells detected by ELISPOT, *Eur. J. Immunol.* 36 (7) (2006) 1772–1781.
- [8] M.W.A. Hussain, S. Jahangir, B. Ghosh, F. Yesmin, A. Anis, S.N. Satil, F. Anwar, M.H. Rashid, Exosomes for regulation of immune responses and immunotherapy, *J. Nanotheranostics* 3 (2022) 55–85.

- [9] S. Ruan, Z. Greenberg, X. Pan, P. Zhuang, N. Erwin, M. He, Extracellular vesicles as an advanced delivery biomaterial for precision cancer immunotherapy, *Adv. Healthc. Mater.* 11 (5) (2022) 2100650.
- [10] Y. Cheng, J.S. Schorey, Exosomes carrying mycobacterial antigens can protect mice against *Mycobacterium tuberculosis* infection, *Eur. J. Immunol.* 43 (12) (2013) 3279–3290.
- [11] J.M. Pitt, F. André, S. Amigorena, J.C. Soria, A. Eggermont, G. Kroemer, L. Zitvogel, Dendritic cell-derived exosomes for cancer therapy, *J. Clin. Invest.* 126 (4) (2016) 1224–1232.
- [12] S. Hong, S. Ruan, Z. Greenberg, M. He, J.L. McGill, Development of surface engineered antigenic exosomes as vaccines for respiratory syncytial virus, *Sci. Rep.* 11 (1) (2021) 21358.
- [13] J. Xia, Y. Miao, X. Wang, X. Huang, J. Dai, Recent progress of dendritic cell-derived exosomes (Dex) as an anti-cancer nanovaccine, *Biomed. Pharmacother.* 152 (2022) 113250.
- [14] C. Théry, L. Duban, E. Segura, P. Véron, O. Lantz, S. Amigorena, Indirect activation of naïve CD4<sup>+</sup> T cells by dendritic cell-derived exosomes, *Nat. Immunol.* 3 (12) (2002) 1156–1162.
- [15] P. Santos, F. Almeida, Exosome-based vaccines: history, current state, and clinical trials, *Front. Immunol.* 12 (2021) 711565.
- [16] B.J. Crenshaw, L. Gu, B. Sims, Q.L. Matthews, Exosome biogenesis and biological function in response to viral infections, *The Open Virology Journal.* 12 (2018) 134.
- [17] Y. Zbrodskaya, M. Plotnikova, N. Gavrilova, A. Lozhkov, S. Klotchenko, A. Kiselev, V. Burdakov, E. Ramsay, L. Purvinsh, M. Egorova, V. Vysochinskaya, I. Baranovskaya, A. Brodskaya, R. Povalikhin, A. Vasin, Exosomes released by influenza-virus-infected cells carry factors capable of suppressing immune defense genes in Naïve cells, *Viruses* 14 (12) (2022) 2690.
- [18] A. Zandifar, R. Badrfam, Iranian mental health during the COVID-19 epidemic, *Asian J. Psychiatr.* 51 (2020) 101990.
- [19] E. Pesce, N. Manfrini, C. Cordiglieri, S. Santi, A. Bandera, A. Gobbi, P. Gruarin, A. Favalli, M. Bombaci, A. Cuomo, F. Collino, G. Cricri, R. Ungaro, A. Lombardi, D. Mangioni, A. Muscatello, S. Aliberti, F. Blasi, A. Gori, S. Abrignani, R. De Francesco, S. Biffo, R. Grifantini, Exosomes recovered from the plasma of COVID-19 patients expose SARS-CoV-2 spike-derived fragments and contribute to the adaptive immune response, *Front. Immunol.* 12 (2022) 785941.
- [20] S.J. Gould, A.M. Booth, J.E. Hildreth, The Trojan exosome hypothesis, *Proc. Natl. Acad. Sci. U. S. A.* 100 (19) (2003) 10592–10597.
- [21] S. Anticoli, F. Manfredi, C. Chiozzini, C. Arenaccio, E. Olivetta, F. Ferrantelli, A. Capocefalo, E. Falcone, A. Ruggieri, M. Federico, An exosome-based vaccine platform imparts cytotoxic T lymphocyte immunity against viral antigens, *Biotechnol. J.* 13 (4) (2018) 1700443.
- [22] R.H. Nanjundappa, R. Wang, Y. Xie, C.S. Umeshappa, R. Chibbar, Y. Wei, Q. Liu, J. Xiang, GP120-specific exosome-targeted T cell-based vaccine capable of stimulating DC- and CD4<sup>+</sup> T-independent CTL responses, *Vaccine* 29 (19) (2011) 3538–3547.
- [23] R.H. Nanjundappa, R. Wang, Y. Xie, C.S. Umeshappa, J. Xiang, Novel CD8<sup>+</sup> T cell-based vaccine stimulates Gp120-specific CTL responses leading to therapeutic and long-term immunity in transgenic HLA-A2 mice, *Vaccine* 30 (24) (2012) 3519–3525.
- [24] R. Wang, A. Xu, X. Zhang, J. Wu, A. Freywald, J. Xu, J. Xiang, Novel exosome-targeted T-cell-based vaccine counteracts T-cell anergy and converts CTL exhaustion in chronic infection via CD40L signaling through the mTORC1 pathway, *Cell. Mol. Immunol.* 14 (6) (2017) 529–545.
- [25] P. Di Bonito, C. Chiozzini, C. Arenaccio, S. Anticoli, F. Manfredi, E. Olivetta, F. Ferrantelli, E. Falcone, A. Ruggieri, M. Federico, Antitumor HPV E7-specific CTL activity elicited by *in vivo* engineered exosomes produced through DNA inoculation, *Int. J. Nanomedicine* 12 (2017) 4579–4591.
- [26] S. Basmaciogullari, M. Pizzato, The activity of Nef on HIV-1 infectivity, *Front. Microbiol.* 5 (2014) 232.
- [27] G.I. Lancaster, M.A. Febbraio, Exosome-dependent trafficking of HSP70: a novel secretory pathway for cellular stress proteins, *J. Biol. Chem.* 280 (24) (2005) 23349–23355.
- [28] R. Gastpar, M. Gehrman, M.A. Bausero, A. Asea, C. Gross, J.A. Schroeder, G. Multhoff, Heat shock protein 70 surface-positive tumor exosomes stimulate migratory and cytolytic activity of natural killer cells, *Cancer Res.* 65 (12) (2005) 5238–5247.
- [29] N. Mouawad, G. Capasso, E. Ruggeri, L. Martinello, F. Severin, A. Visentin, M. Facco, L. Trentin, F. Frezzato, Is it still possible to think about HSP70 as a therapeutic target in onco-hematological diseases? *Biomolecules* 13 (4) (2023) 604.
- [30] E.Y. Komarova, R.V. Suezov, A.D. Nikotina, N.D. Aksenov, L.A. Garaeva, T. A. Shtam, A.V. Zhakhov, M.G. Martynova, O.A. Bystrova, M.S. Istomina, A. M. Ischenko, B.A. Margulis, I.V. Guzova, Hsp70-containing extracellular vesicles are capable of activating of adaptive immunity in models of mouse melanoma and colon carcinoma, *Sci. Rep.* 11 (1) (2021) 21314.
- [31] S. Alipour, A. Mahdavi, Boosting tat DNA vaccine with tat protein stimulates strong cellular and humoral immune responses in mice, *Biotechnol. Lett.* 42 (2020) 505–517.
- [32] B. Romani, S. Engelbrecht, R.H. Glashoff, Functions of tat: the versatile protein of human immunodeficiency virus type 1, *J. Gen. Virol.* 91 (1) (2010) 1–12.
- [33] S. Bayanolhagh, M. Alinezhad, K. Kamali, M. Foroughi, H.R. Khorram Khorshid, M. Mohraz, F. Mahboudi, A.A. Pourfathollah, Characterization of immune responses induced by combined Clade-A HIV-1 recombinant Adenovectors in mice, *Iran. J. Immunol.* 7 (3) (2010) 162–176.
- [34] A. Cafaro, A. Tripiciano, O. Picconi, C. Sgadari, S. Moretti, S. Buttò, P. Monini, B. Ensoli, Anti-tat immunity in HIV-1 infection: effects of naturally occurring and vaccine-induced antibodies against tat on the course of the disease, *Vaccines* 7 (3) (2019) 99.
- [35] M.K. Kim, J. Kim, Properties of immature and mature dendritic cells: phenotype, morphology, phagocytosis, and migration, *RSC Adv.* 9 (20) (2019) 11230–11238.
- [36] S. Chopra, P. Ruzgys, M. Maciulevičius, M. Jakutavičiūtė, S. Šatkauskas, Investigation of plasmid DNA delivery and cell viability dynamics for optimal cell electrotransfection *in vitro*, *Appl. Sci.* 10 (17) (2020) 6070.
- [37] N. Schaft, J. Dörrie, P. Thumann, V.E. Beck, I. Müller, E.S. Schultz, E. Kämpgen, D. Dieckmann, G. Schuler, Generation of an optimized polyvalent monocyte-derived dendritic cell vaccine by transfecting defined RNAs after rather than before maturation, *J. Immunol.* 174 (5) (2005) 3087–3097.
- [38] S. Yu, C. Liu, K. Su, J. Wang, Y. Liu, L. Zhang, C. Li, Y. Cong, R. Kimberly, W. E. Grizzle, C. Falkson, Tumor exosomes inhibit differentiation of bone marrow dendritic cells, *J. Immunol.* 178 (11) (2007) 6867–6875.
- [39] M. Tkach, J. Kowal, A.E. Zucchetti, L. Enserink, M. Jouve, D. Lankar, M. Saitakis, L. Martin-Jaular, C. Théry, Qualitative differences in T-cell activation by dendritic cell-derived extracellular vesicle subtypes, *EMBO J.* 36 (20) (2017) 3012–3028.
- [40] J.K. Schnitzer, S. Berzel, M. Fajardo-Moser, K.A. Remer, H. Moll, Fragments of antigen-loaded dendritic cells (DC) and DC-derived exosomes induce protective immunity against *Leishmania major*, *Vaccine* 28 (36) (2010) 5785–5793.
- [41] E. Akbari, S. Ajdary, E. Mirabzadeh Ardakani, E. Agi, A. Milani, M. Seyedinkhorasani, V. Khalaj, A. Bolhassani, Immunopotentiality by linking Hsp70 T-cell epitopes to Gag-Pol-Env-Nef-Rev multipeptide construct and increased IFN-gamma secretion in infected lymphocytes, *Pathogens and Disease* 80 (2022) 1–11.
- [42] A. Namvar, H.A. Panahi, E. Agi, A. Bolhassani, Development of HPV16,18,31,45 E5 and E7 peptides-based vaccines predicted by immunoinformatics tools, *Biotechnol. Lett.* 42 (2020) 403–418.
- [43] E. Avc, B. Balç-Peynircioğlu, An overview of exosomes: from biology to emerging roles in immune response, *Acta Med. Austriaca* 47 (1) (2016) 2–10.
- [44] M.A. Navarrete-Muñoz, C. Llorens, J.M. Benito, N. Rallón, Extracellular vesicles as a new promising therapy in HIV infection, *Front. Immunol.* 12 (2022) 811471.
- [45] G.H. Mylvaganam, G. Silvestri, R.R. Amara, HIV therapeutic vaccines: moving towards a functional cure, *Curr. Opin. Immunol.* 35 (2015) 1–8.
- [46] S. Shrivastava, R.M. Ray, L. Holguin, L. Echavarría, N. Grepo, T.A. Scott, J. Burnett, K.V. Morris, Exosome-mediated stable epigenetic repression of HIV-1, *Nat. Commun.* 12 (1) (2021) 5541.
- [47] S. Bhatnagar, J.S. Schorey, Exosomes released from infected macrophages contain *Mycobacterium avium* glycopeptidolipids and are proinflammatory, *J. Biol. Chem.* 282 (35) (2007) 25779–25789.
- [48] J.D. Walker, C.L. Maier, J.S. Pober, Cytomegalovirus-infected human endothelial cells can stimulate allogeneic CD4<sup>+</sup> memory T cells by releasing antigenic exosomes, *J. Immunol.* 182 (3) (2009) 1548–1559.
- [49] L. Zitvogel, A. Regnault, A. Lozier, J. Wolfers, C. Flament, D. Tenza, P. Ricciardi-Castagnoli, G. Raposo, S. Amigorena, Eradication of established murine tumors using a novel cell-free vaccine: dendritic cell derived exosomes, *Nat. Med.* 4 (1998) 594–600.
- [50] M. Tkach, J. Kowal, C. Théry, Why the need and how to approach the functional diversity of extracellular vesicles, *Philos. Trans. R. Soc., B* 373 (1737) (2018) 20160479.
- [51] M. Tkach, J. Kowal, A.E. Zucchetti, L. Enserink, M. Jouve, D. Lankar, M. Saitakis, L. Martin-Jaular, C. Théry, Qualitative differences in T-cell activation by dendritic cell-derived extracellular vesicle subtypes, *EMBO J.* 36 (20) (2017) 3012–3028.
- [52] W.W. Hui, L.E. Emerson, B. Clapp, A.E. Sheppe, J. Sharma, J. Del Castillo, M. Ou, G.H.B. Maegawa, C. Hoffman, J.L. Iii, D.W. Pascual, M.J. Ferraro, Antigen-encapsulating host extracellular vesicles derived from *Salmonella*-infected cells stimulate pathogen-specific Th1-type responses *in vivo*, *PLoS Pathog.* 17 (5) (2021) e1009465.
- [53] M.N. Huda, M. Nurunnabi, Potential application of exosomes in vaccine development and delivery, *Pharm. Res.* 39 (11) (2022) 2635–2671.
- [54] Y. Cheng, J.S. Schorey, Exosomes carrying mycobacterial antigens can protect mice against *Mycobacterium tuberculosis* infection, *Eur. J. Immunol.* 43 (12) (2013) 3279–3290.
- [55] P. Santos, F. Almeida, Exosome-based vaccines: history, current state, and clinical trials, *Front. Immunol.* 12 (2021) 711565.
- [56] K. Kardani, A. Milani, A. Bolhassani, Gene delivery in adherent and suspension cells using the combined physical methods, *Cytotechnology* 74 (2) (2022) 245–257.
- [57] L.C. Parr-Brownlie, C. Bosch-Bouju, L. Schoderboeck, R.J. Sizemore, W. C. Abraham, S.M. Hughes, Lentiviral vectors as tools to understand central nervous system biology in mammalian model organisms, *Front. Mol. Neurosci.* 8 (2015) 14.
- [58] J. Jakobsson, C. Lundberg, Lentiviral vectors for use in the central nervous system, *Mol. Ther.* 13 (3) (2006) 484–493.
- [59] A.M. Munis, Gene therapy applications of non-human lentiviral vectors, *Viruses* 12 (10) (2020) 1106.
- [60] H.A. Tomás, A.F. Rodrigues, P.M. Alves, A.S. Coroadinha, Lentiviral gene therapy vectors: challenges and future directions, *IntechOpen* (2013) 287–317.
- [61] J.E. Vargas, L. Chicaybam, R.T. Stein, A. Tanuri, A. Delgado-Cañedo, M. H. Bonamino, Retroviral vectors and transposons for stable gene therapy: advances, current challenges and perspectives, *J. Transl. Med.* 14 (1) (2016) 1–15.

- [62] S. Ghosh, A.M. Brown, C. Jenkins, K. Campbell, Viral vector systems for gene therapy: a comprehensive literature review of progress and biosafety challenges, *Applied Biosafety* 25 (1) (2020) 7–18.
- [63] H. Potter, R. Heller, Transfection by electroporation, *Curr. Protoc. Mol. Biol.* 121 (1) (2018), 9.3.1–9.3.13.
- [64] T. Kotnik, L. Rems, M. Tarek, D. Miklavčič, Membrane electroporation and electropermeabilization: mechanisms and models, *Annu. Rev. Biophys.* 48 (2019) 63–91.
- [65] Z. Zhang, S. Qiu, X. Zhang, W. Chen, Optimized DNA electroporation for primary human T cell engineering, *BMC Biotechnol.* 18 (2) (2022) 1–9.
- [66] J.J. Sherba, S. Hogquist, H. Lin, J.W. Shan, D.I. Shreiber, J.D. Zahn, The effects of electroporation buffer composition on cell viability and electro-transfection efficiency, *Sci. Rep.* 10 (1) (2020) 3053.
- [67] E. Yakubovich, A. Polischouk, V. Evtushenko, Principles and problems of exosome isolation from biological fluids, *biochemistry (Moscow), Supplement Series A: Membrane and Cell Biology* 16 (2) (2022) 115–126.
- [68] G.G. Diaz-Armas, A.P. Cervantes-Gonzalez, R. Martinez-Duarte, V.H. Perez-Gonzalez, Electrically driven microfluidic platforms for exosome manipulation and characterization, *Electrophoresis* 43 (1–2) (2022) 327–339.
- [69] C.J. Wahlund, G. Güclülür, S. Hiltbrunner, R.E. Veerman, T.I. Näslund, S. Gabrielsson, Exosomes from antigen-pulsed dendritic cells induce stronger antigen-specific immune responses than microvesicles *in vivo*, *Sci. Rep.* 7 (1) (2017) 17095.
- [70] S. Gurung, D. Perocheau, L. Touramanidou, J. Baruteau, The exosome journey: from biogenesis to uptake and intracellular signalling, *Cell Communication and Signaling* 19 (1) (2021) 1–19.
- [71] V.L. Ferreira, H.H. Borba, A.F. Bonetti, L. Leonart, R. Pontarolo, Cytokines and interferons: types and functions, *Autoantibodies and Cytokines* 13 (2018) 1–25.
- [72] Y. Huang, K.E. Seaton, M. Casapia, L. Polakowski, S.C. De Rosa, K. Cohen, NIAID-funded HIV vaccine trials network (HVTN) 114 study team, AIDSvax protein boost improves breadth and magnitude of vaccine-induced HIV-1 envelope-specific responses after a 7-year rest period, *Vaccine* 39 (33) (2021) 4641–4650.
- [73] Y. Huang, G. Pantaleo, G. Tapia, B. Sanchez, L. Zhang, M. Trondsen, A.O. Hovden, R. Pollard, J. Rockstroh, M. Ökvist, M.A. Sommerfelt, Cell-mediated immune predictors of vaccine effect on viral load and CD4 count in a phase 2 therapeutic HIV-1 vaccine clinical trial, *EBioMedicine* 24 (2017) 195–204.
- [74] P.D. Katsikis, Y.M. Mueller, F. Villingier, The cytokine network of acute HIV infection: a promising target for vaccines and therapy to reduce viral set-point? *PLoS Pathog.* 7 (8) (2011) e1002055.
- [75] B.R. Lane, D.M. Markovitz, N.L. Woodford, R. Rochford, R.M. Strieter, M. J. Coffey, TNF- $\alpha$  inhibits HIV-1 replication in peripheral blood monocytes and alveolar macrophages by inducing the production of RANTES and decreasing CC chemokine receptor 5 (CCR5) expression, *J. Immunol.* 163 (7) (1999) 3653–3661.
- [76] M.F. Lindenbergh, R. Wubbolts, E.G. Borg, E.M. van't Veld, M. Boes, W. Stoorvogel, Dendritic cells release exosomes together with phagocytosed pathogen; potential implications for the role of exosomes in antigen presentation, *J. Extracellular Vesicles* 9 (1) (2020) 1798606.
- [77] B.B. Shenoda, S.K. Ajit, Modulation of immune responses by exosomes derived from antigen-presenting cells, *Clinical Medicine Insights: Pathology* 9 (2016) S39925.
- [78] B. Shen, N. Wu, J.M. Yang, S.J. Gould, Protein targeting to exosomes/microvesicles by plasma membrane anchors, *J. Biol. Chem.* 286 (16) (2011) 14383–14395.
- [79] Y. Yao, C. Fu, L. Zhou, Q.S. Mi, A. Jiang, DC-derived exosomes for cancer immunotherapy, *Cancers* 13 (15) (2021) 3667.
- [80] Y. Wang, Y. Xiang, V.W. Xin, X.W. Wang, X.C. Peng, X.Q. Liu, D. Wang, N. Li, J. T. Cheng, Y.N. Lyv, S.Z. Cui, Z. Ma, Q. Zhang, H.W. Xin, Dendritic cell biology and its role in tumor immunotherapy, *J. Hematol. Oncol.* 13 (1) (2020) 1–18.
- [81] E.I. Buzas, The roles of extracellular vesicles in the immune system, *Nat. Rev. Immunol.* 23 (4) (2023) 236–250.
- [82] R. Kulkarni, A. Prasad, Exosomes derived from HIV-1 infected DCs mediate viral trans-infection via fibronectin and galectin-3, *Sci. Rep.* 7 (1) (2017) 14787.
- [83] P. Gangadaran, H. Madhyastha, R. Madhyastha, R.L. Rajendran, Y. Nakajima, N. Watanabe, A.K.G. Velikkakath, C.M. Hong, R.V. Gopi, G.K. Muthukalianan, A. V. Gopalakrishnan, M. Jeyaraman, B.C. Ahn, The emerging role of exosomes in innate immunity, diagnosis and therapy, *Front. Immunol.* 13 (2023) 1085057.
- [84] D.H. Kim, V.K. Kothandan, H.W. Kim, K.S. Kim, J.Y. Kim, H.J. Cho, Y.K. Lee, D. E. Lee, S.R. Hwang, Noninvasive assessment of exosome pharmacokinetics *in vivo*: a review, *Pharmaceutics* 11 (12) (2019) 649.
- [85] H. Choi, Y. Choi, H.Y. Yim, A. Mirzaaghasi, J.K. Yoo, C. Choi, Biodistribution of exosomes and engineering strategies for targeted delivery of therapeutic exosomes, *Tissue Engineering and Regenerative Medicine* 18 (4) (2021) 499–511.
- [86] M.A. Reuter, C. Pombo, M.R. Betts, Cytokine production and dysregulation in HIV pathogenesis: lessons for development of therapeutics and vaccines, *Cytokine Growth Factor Rev.* 23 (4–5) (2012) 181–191.
- [87] B. Sabanovic, F. Piva, M. Cecati, M. Giuliotti, Promising extracellular vesicle-based vaccines against viruses including SARS-CoV-2, *Biology* 10 (2) (2021) 94.
- [88] A. Harari, M. Graciotti, M. Bassani-Sternberg, L.E. Kandalaft, Antitumor dendritic cell vaccination in a priming and boosting approach, *Nat. Rev. Drug Discov.* 19 (9) (2020) 635–652.
- [89] K.R. Qazi, U. Gehrman, E. Domange Jordö, M.C. Karlsson, S. Gabrielsson, Antigen-loaded exosomes alone induce Th1-type memory through a B cell-dependent mechanism, *Blood: The Journal of the American Society of Hematology* 113 (12) (2009) 2673–2683.
- [90] H. Zhu, K. Wang, Z. Wang, D. Wang, X. Yin, Y. Liu, F. Yu, W. Zhao, An efficient and safe MUC1-dendritic cell-derived exosome conjugate vaccine elicits potent cellular and humoral immunity and tumor inhibition *in vivo*, *Acta Biomater.* 138 (2022) 491–504.
- [91] K. Hu, P.F. McKay, K. Samnuan, A. Najer, A.K. Blakney, J. Che, G. O'Driscoll, M. Cihova, M.M. Stevens, R.J. Shattock, Presentation of antigen on extracellular vesicles using transmembrane domains from viral glycoproteins for enhanced immunogenicity, *J. Extracellular Vesicles* 11 (3) (2022) e12199.
- [92] J. Fornefelt, J. Krause, K. Klose, F. Pingas, R. Hassert, L. Benga, T. Grunwald, U. Müller, W. Schrödl, C.G. Baums, Comparative analysis of humoral immune responses and pathologies of BALB/c and C57BL/6 wildtype mice experimentally infected with a highly virulent *Rodentibacter pneumotropicus* (*Pasteurella pneumotropica*) strain, *BMC Microbiol.* 18(1) (2018) 1–11.
- [93] D.H. Cribbs, A. Ghochikyan, V. Vasilevko, M. Tran, I. Petrushina, N. Sadzikava, D. Babikyan, P. Kesslak, T. Kieber-Emmons, C.W. Cotman, M.G. Agadjanyan, Adjuvant-dependent modulation of Th1 and Th2 responses to immunization with  $\beta$ -amyloid, *Int. Immunol.* 15 (4) (2003) 505–514.
- [94] J.B. McBrien, N.A. Kumar, G. Silvestri, Mechanisms of CD8+ T cell-mediated suppression of HIV/SIV replication, *Eur. J. Immunol.* 48 (6) (2018) 898–914.
- [95] C. Zhang, W. Hu, J. Jin, M. Zhou, J. Song, J. Deng, L. Huang, S.Y. Wang, F. S. Wang, The role of CD8 T cells in controlling HIV beyond the antigen-specific face, *HIV Med.* 21 (11) (2020) 692–700.
- [96] T.M. Ta, S. Malik, E.M. Anderson, A.D. Jones, J. Perchik, M. Freylikh, L. Sardo, Z. A. Klase, T. Izumi, Insights into persistent HIV-1 infection and functional cure: novel capabilities and strategies, *Front. Microbiol.* 13 (2022) 862270.
- [97] W.J. Grossman, J.W. Verbsky, B.L. Tollefsen, C. Kemper, J.P. Atkinson, T.J. Ley, Differential expression of granzymes A and B in human cytotoxic lymphocyte subsets and T regulatory cells, *Blood* 104 (9) (2004) 2840–2848.
- [98] S. Mellor-Heineke, J. Villanueva, M.B. Jordan, R. Marsh, K. Zhang, J.J. Bleesing, A.H. Filipovich, K.A. Risma, Elevated granzyme B in cytotoxic lymphocytes is a signature of immune activation in hemophagocytic lymphohistiocytosis, *Front. Immunol.* 4 (2013) 72.
- [99] C. Sbarigia, D. Vardanyan, L. Buccini, S. Tacconi, L. Dini, SARS-CoV-2 and extracellular vesicles: an intricate interplay in pathogenesis, diagnosis and treatment, *Front. Nanotechnol.* 4 (2022) 987034.
- [100] M. Krupka, K. Zachova, R. Cahlikova, J. Vrbkova, Z. Novak, M. Sebel, E. Weigl, M. Raska, Endotoxin-minimized HIV-1 p24 fused to murine hsp70 activates dendritic cells, facilitates endocytosis and p24-specific Th1 response in mice, *Immunol. Lett.* 166 (1) (2015) 36–44.
- [101] M.W.A. Hussain, S. Jahangir, B. Ghosh, F. Yesmin, A. Anis, S.N. Satil, F. Anwar, M.H. Rashid, Exosomes for regulation of immune responses and immunotherapy, *J. Nanotheranostics* 3 (1) (2022) 55–85.